2011

DRE-1/FBXO11, A Conserved F Box Protein, Regulates Apoptosis in C. elegans and is Mutated in Human Lymphoma

Michael Chiorazzi

DRE-1/FBXO11, A CONSERVED F BOX PROTEIN, REGULATES APOPTOSIS IN *C. ELEGANS* AND IS MUTATED IN HUMAN LYMPHOMA

A Thesis Presented to the Faculty of

The Rockefeller University

in Partial Fulfillment of the Requirements for

the degree of Doctor of Philosophy

by

Michael Chiorazzi

June 2011

DRE-1/FBXO11, a conserved F box protein, regulates apoptosis in *C. elegans* and is mutated in human lymphoma

Michael Chiorazzi, Ph.D.

The Rockefeller University 2011

In the course of metazoan embryonic and post-embryonic development, more cells are generated than exist in the mature organism, and these cells are deleted by the process of programmed cell death. In addition, cells can be pushed toward death when they accumulate genetic errors, are virally-infected or are otherwise deemed potentially-harmful to the overall organism. *Caenorhabditis elegans* has proved to be an excellent model system for elucidating the genetic underpinnings of cell death, and research has shown that the core machinery, made up of the *egl-1*, *ced-9*, *ced-4* and *ced-3* genes, is conserved across metazoans, and their homologues are crucial for such diseases as cancer, neurodegeneration and autoimmunity. We used the *C. elegans* tail-spike cell as a model to uncover *dre-1*/FBXO11 as a conserved

apoptotic regulator that controls tail-spike cell death and also plays a role in human lymphoma.

The tail-spike cell is unique among cells fated for programmed cell death in two ways. First, unlike most dying *C. elegans* cells, the tail-spike cell lives for several hours before its demise, and during this time differentiates. In comparison, most cells die minutes after birth as undifferentiated cells. Second, while tail-spike cell death requires both the CED-3 caspase and CED-4/Apaf-1 adaptor proteins, the BH3-only protein EGL-1 is dispensable. Thus, other gene(s) substitute for *egl-1*'s role as a regulator of caspase activation in this cell, and we set out to identify the relevant gene or genes.

A screen for mutants in which the tail-spike cell survives inappropriately yielded a mutant, *ns39*, in which the *ced-3* caspase is transcribed as normal, but fails to become activated. We mapped and cloned this mutant, and found that *dre-1* (*daf-12-redundant-1*) is required for caspase activation in the tail-spike cell. Expression of the *dre-1* cDNA in the tail-spike cell rescues the *dre-1(ns39)* defect in a cell autonomous manner, and expression studies show that *dre-1* is expressed in the tail-spike cell. Partial loss-of-function alleles of *dre-1*, when combined with weak loss-of-function alleles of *ced-3* and *ced-4*, a null allele of *egl-1*, or a weak gain-of-function allele of *ced-9* exhibit a synergistic loss of tail-spike cell death. A null allele of *ced-9*, however, when combined with a strong loss-of-function *dre-1* allele, suppresses the tail-spike cell death phenotype of the *dre-1(ns39)*. This epistatic relationship shows that *dre-1* acts upstream of, or in

parallel to *ced-9*. These results show that *dre-1* has a central role in tail-spike cell death, and are consistent with it acting in place of *egl-1* to promote tail-spike cell death.

DRE-1 is an F box protein, and we showed via RNAi and genetic experiments that DRE-1 acts in an SCF complex with CUL-1 and SKR-1 to regulate tail-spike cell death, and present evidence that DRE-1 and CED-9 bind to each other *in vitro*. These results suggest a model in which the *dre-1* SCF complex ubiquitinates CED-9 to eliminate its anti-apoptotic function and open the way for the cell to die.

A collaboration with Louis Staudt and Lixin Rui at the National Cancer Institute revealed that *dre-1*'s human homologue, FBXO11 is mutated or deleted in 5% of germinal center-like diffuse large B cell lymphomas, and that reintroduction of the gene into lymphoma cell lines that have deleted it induces apoptosis. In addition, FBXO11 binds to BCL2 in lymphoma cell lines and induces the degradation of BCL2, and expression of BCL2 rescues the toxicity of FBXO11.

Taken together, our results establish *dre-1*/FBXO11 as a regulator of apoptosis in *C. elegans* and human lymphoma, and suggest a model in which DRE-1/FBXO11 ubiquitinates and degrades BCL2, a major anti-apoptotic protein.

Acknowledgments

I owe a great debt of gratitude to Shai Shaham, my advisor. One of his salient qualities as a mentor is his scientific curiosity, which I strive to always emulate. He is always available for his lab members, and he has a way of asking the incisive question that cuts to the heart of the matter. Without his ideas and guidance, this work would not have been possible.

Thank you also to my committee members, Hermann Steller, Jim Darnell, Xuejun Jiang and Monica Driscoll. Their advice and questions have proved invaluable over the course of my project.

We are grateful to Lou Staudt, who had the curiosity and took the time to look for evidence of a role for FBXO11 in human lymphoma, and also to Lixin Rui for his skilled work in elucidating the mechanisms of this role.

This work could not have been completed without the support and advice of the entire Shaham lab, an always-friendly environment for science. In particular, I want to thank Maya Tevlin, who has taught me so much, from how to

pick worms to how to think creatively about science, while, above all, being a great friend every day. Also, a special thanks to Max Heiman, who has never hesitated to take time out of his own work to talk about scientific issues large and small. He has a special ability to communicate about science, something I have tried to learn.

Thank you as well to my family, who have given me the utmost support over these past few years and for my entire life. I first became fascinated with science at my father's lab bench in Founder's Hall as a 6 year-old, when I was astounded by the change of color in an ELISA assay. I trace the excitement I derive from science back to that spark he gave me as a boy.

Finally, I am indebted to my wife, Shelli. I could not ask for a more generous, intelligent and caring partner, or for a better friend.

Table of Contents

List of Figures

List of Tables

Chapter 1: Introduction

In the development of nearly all metazoans, more cells are generated than exist in the mature animal, and these cells extra cells are fated to die by the process known as programmed cell death or apoptosis. While developmental cell deaths were first observed in the 19th century, the appreciation that these were a normal facet of producing a multicellular organism did not arrive until Glucksmann's work in the 1950s (Glucksmann, 1951). His descriptive review set the stage for future studies on apoptosis.

Genetic control of programmed cell death

A major advance in understanding the genetic basis of this process came in H. Robert Horvitz's lab in the 1980s and 90s, when the first genetic mutants were isolated in which cell deaths failed to occur. Sulston and Horvitz (Sulston and Horvitz, 1977) had recognized that Nomarski differential interference contrast microscopy could be used to identify dying cells as they become round corpses.

A screen in a *ced-1* engulfment-defective background, in which corpses persist and are easily identified, yielded the *ced-3(n717)* mutant, in which nearly all cell deaths are eliminated, yet no changes occur in the stereotyped cell lineage (Ellis and Horvitz, 1986). *egl-1* had been previously isolated and recognized to involve deaths of the hermaphrodite-specific neurons (HSNs) that control egg-laying, and *ced-4(n1162)* was isolated as a suppressor of *egl-1(n1084)* (Ellis and Horvitz, 1986). Finally, *ced-9* was isolated as a gain-of-function allele in a similar screen for inappropriate survival, and was shown to act as an anti-apoptotic gene (Hengartner et al., 1992). These results defined *C. elegans* as an ideal system for identifying cell death regulators, established the counting of extra cells in the anterior pharynx as a technique for assessing cell death, and ordered these genes into a genetic pathway (Fig. 1).

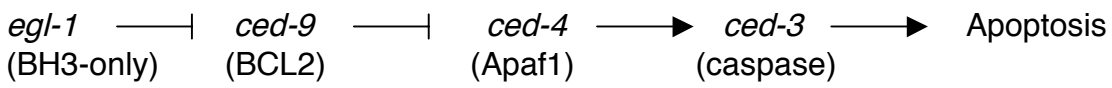

Fig. 1. The core cell death machinery in *C. elegans* and their vertebrate homologues.

When the molecular identities of the core apoptotic machinery were elucidated, the field had its first inklings of what the mechanism of cell death might be, and that these genes were conserved in sequence and function across metazoans (Conradt and Horvitz, 1998; Hengartner et al., 1992; Yuan and

Horvitz, 1992; Yuan et al., 1993). *ced-3* was found to encode a cysteine protease, similar to the vertebrate interleukin-1β-converting enzyme (Yuan et al., 1993). A novel class of proteins was identified with the cloning of *ced-4* (Yuan and Horvitz, 1992), but later was found to be homologous to the mammalian Apaf-1 gene (Zou et al., 1997). BCL2 had been previously cloned as the gene translocated to the immunoglobulin locus in human follicular lymphoma, and shown to prevent cell death in B cells and T cells (Tsujimoto et al., 1984; Vaux et al., 1988). Thus, the connection to BCL2 was immediately made when *ced-9*, its homologue, was identified (Hengartner et al., 1992) and further when the molecular nature of *ced-9(n1950)* was elucidated (Hengartner and Horvitz, 1994). Finally, when *egl-1* was identified and shown to be a pro-apoptotic gene containing a BCL2-homology-3 (BH3) domain, it fit well with the cloning in the preceding years of several mammalian cell death activators with BH3 domains: Bid, Bad, Bax and Bak. Thus, the *C. elegans* core apoptotic machinery was identified and models for its function were proposed and later validated.

The current model for activation of programmed cell death in *C. elegans* (Fig. 2) begins with a cell not yet fated to die, in which CED-9 protein is tethered to the mitochondrial outer membrane, and a CED-4 dimer is being held inactive by CED-9. This complex prevents CED-4 from binding to inactive CED-3, which is cytosolic and most-likely inherited (Maurer et al., 2007). Thus the cell has the potential to undergo apoptosis, but remains alive until an initiating stimulus induces its death (Shaham and Horvitz, 1996a). When EGL-1 is expressed, it

binds to CED-9, inducing a conformational change that results in the release of CED-4. Now free from CED-9 inhibition, CED-4 forms a higher order structure, the “apoptosome” which binds to cytosolic CED-3, bringing the protease into position to be cleaved and become active. Active CED-3 further cleaves CED-3 zymogens and soon, through a feed forward mechanism, all CED-3 becomes active. The active protease cleaves cellular proteins after aspartate residues, rapidly dismantling the cell.

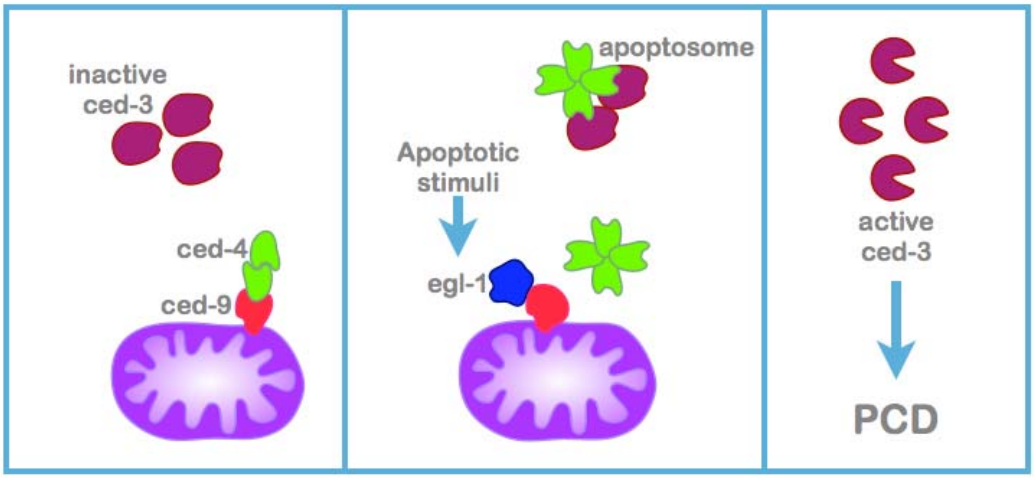

Fig. 2. The current model for the apoptotic pathway in *C. elegans*.
In most or all cells, inactive CED-3 zymogen is available in the cytosol, while CED-9 is tethered to the mitochondrial membrane and holds CED-4 inactive. Once the apoptotic pathway is engaged, *egl-1* is transcribed. The EGL-1 protein binds to CED-9, releasing CED-4, which forms an oligomer. This complex associates with CED-3, leading to its proteolytic cleavage and activation. Active CED-3 dismantles the cell.

The tail-spike cell as a model for investigating programmed cell death

John Sulston, in his landmark paper, *The Embryonic Cell Lineage of the Nematode Caenorhabditis elegans*, described his observations regarding cell death:

"In the course of the lineage, one in six of all cells produced subsequently dies; their identity and the approximate times of their deaths are predictable. The mode of death is similar to that seen previously in the postembryonic lineages. In some cases death occurs several hours after birth, so that it is possible for the cells to function in some manner before being discarded. A good example is the pair of tail spike cells, which fuse together, form a slender bundle of filaments in the tip of the tail, and then die. At the other extreme are the majority of programmed deaths, which occur 20 to 30 min after birth; these cells are born with very little cytoplasm, and die without differentiating in any obvious way (Sulston et al., 1983)."

Sulston's short paragraph forms the foundation for this thesis project. Because screens for global cell death regulators have already been carried out, we chose to study the death of an individual cell, with the hope of uncovering novel regulators of apoptosis. But which one to choose? The tail-spike cell was an inviting model for the reasons suggested by Sulston. First, the cell appears to have a function before its death – to pattern its sister cell, hyp10, by extending a process into the tail spike around which hyp10 is wrapped. Second, the tail-spike cell is unique in its morphology as well as in the timing of its death. Most cell

deaths occur in small, undifferentiated cells with very little cytoplasm, and death occurs almost immediately after the birth of the cell. These small cells are most likely produced by asymmetric cell division and have no function in the animal. The tail-spike cell, on the other hand, lives about 10 times as long and is thus similar to cells that die in mammals and other organisms, where the majority of deaths occur in differentiated cells that receive a signal to die. Thus, what we learn about tail-spike cell death may be more relevant to cell death biology outside *C. elegans*; many developmental deaths in vertebrates occur in cells that have lived for a long period of time and differentiated fully (Meier et al., 2000).

Following Sulston's description above, electron micrographs confirmed the anatomy of hyp10 and the tail-spike cell, but the tail-spike cell was not studied until recently, when Carine Maurer undertook its study as a model for understanding cell death. The first step in understanding tail-spike cell death was to develop a specific fluorescent marker for the cell so that its status as alive or dead could be readily assessed. While a 1.5 kb promoter fragment from the *ced-3* gene drove GFP expression in the cell, it also led to inappropriate survival in many animals, presumably by preventing endogenous *ced-3* transcription in the cell. Using a 690 bp fragment of the *C. briggsae ced-3* gene retained the GFP expression but also eliminated the cell death defect. This transgene was integrated and carries the name *nsIs25*. It was used in all remaining tail-spike cell studies.

With a simple assay for tail-spike cell death, i.e., presence or absence of the GFP-labeled cell, genetic mutants could be used to determine which genes are required for tail-spike cell death. Like most cell deaths in the worm, *ced-3* and *ced-4* were required for this cell to die; 100% of animals harboring null mutations in *ced-3* or *ced-4* had inappropriately surviving tail-spike cells. While this result was unsurprising, that *egl-1* is not required was unexpected. In *egl-1* null animals, 30% of animals had a surviving tail-spike cell, compared to a complete block in pharyngeal cell death. This result points out that the tail-spike cell is an interesting model for another reason beyond Sulston's initial observations: even in the absence of *egl-1* activity, the tail-spike cell is able to "know" that it is fated for death and to execute that death normally in 70% of animals. *egl-1* is not required for germline cell death (Gumienny et al., 1999), but does control the vast majority of somatic deaths by inhibiting *ced-9*. In the tail-spike cell, however, other gene(s) must serve *egl-1*'s function as an upstream control of apoptosis. Maurer et al. also showed that the residual *egl-1* activity, though comparatively minor, fully requires *ced-9* for its function; *ced-9;egl-1* double mutants had 0% tail-spike cell survival, showing that *egl-1* acts through *ced-9* in the tail-spike cell. In addition, the *ced-9* gain-of-function allele *n1950* has a weak effect on tail-spike cell death (3% survival), suggesting that, again, the tail-spike cell is unique in its cell death mechanisms (Maurer et al., 2007).

Analysis of the *ced-3* promoter identified three regions conserved between *C. elegans* and *C. briggsae* that are required for *ced-3pro::gfp* expression in the

tail-spike cell and induction of cell death. A screen for lack of *ced-3pro::gfp* expression in the tail-spike cell identified several mutants, including two, *ns114* and *ns115*, that mapped to the homeodomain transcription factor *pal-1*. In these mutants, *ced-3* transcription was reduced, leading to weaker or no GFP expression as well as inappropriate survival of the tail-spike cell. Electrophoretic mobility shift assays showed that *pal-1* binds to the *ced-3* promoter in two of the regions required for tail-spike cell *ced-3pro::gfp* expression, suggesting that *pal-1* regulates tail-spike cell death by inducing *ced-3* transcription during late embryogenesis, and providing the downstream cue for the cell to die (Maurer et al., 2007). Intriguingly, *pal-1* is homologous to mouse Cdx2 which has been shown to be a tumor suppressor in mouse gut (Aoki et al., 2003; Bonhomme et al., 2003).

The ubiquitin proteasome system and its role in cell death regulation

All biologic processes at their core are chemical reactions, and, as any high school chemistry student knows, the concentrations of reactants and products are crucial to determining which reactions will occur and how quickly. Thus, it is not surprising that much of biological regulation occurs via perturbations of protein levels. For the purposes of increasing protein amounts, a vast array of mechanisms have evolved: transcription factors, chromatin modifications, mRNA trafficking, nuclear receptors and more. Fewer modes exist

for eliminating proteins, and one system is dominant, perhaps because of the specificity it imparts: the ubiquitin-proteasome system.

Ubiquitin-mediated protein degradation consists of two steps: first, a target protein is covalently modified with a chain of ubiquitin molecules; second, the 26S proteasome uses ATP to proteolyze it. In addition to the proteasome and ubiquitin, E1, E2 and E3 enzymes are required, and these may be single molecules or multi-subunit complexes. Initially, a ubiquitin monomer is covalently conjugated to a cysteine residue on one of the few E1s (only one exists in *C. elegans*, *uba-1*). This reaction requires ATP. The ubiquitin is then transferred to an E2, of which there are more in most genomes; in the human there are about 20 and in the *C. elegans* genome there are 22 *ubc* genes. Finally, the ubiquitin is conjugated to its target protein in a reaction that is catalyzed by the E3, the substrate-specificity protein. Because of this specificity requirement, a huge number of E3s have been identified in genomes, including hundreds in humans (Hicke et al., 2005; Hoeller et al., 2006). Ubiquitin's C-terminal glycine is attached with an isopeptide bond to a lysine on the target molecule, followed by repeated conjugations until a polyubiquitin chain is produced; at least four ubiquitin monomers are required for trafficking to the proteasome.

The proteasome is a large, multi-subunit complex made up of a 20S core and two 19S regulatory subunits. The 20S core contains four stacked rings made up of seven α subunits in the two outer rings and seven β subunits in the inner rings (Besche et al., 2009). On the inside surface of the cylinder are six

proteolytic sites that have chymotrypsin-like, trypsin-like and peptidylglutamyl peptide hydrolytic activities; these active sites digest the substrates into 7-9 residue peptides (Voges et al., 1999).

Because the proteasome is an efficient means to destroy cellular contents, its gating must be tightly controlled. The gating mechanism involves the N-terminal tails of the α subunits which extend into the central pore and block its opening until the 19S regulatory particle induces their opening (Groll et al., 2000). This ungating requires ATP hydrolysis through the six ATPase subunits of the 19S particle. In addition, ATP is required for unfolding of the target protein and for its entry into the core (Smith et al., 2005). The 19S regulatory subunit binds to the polyubiquitin chain, and this transduces opening of the 20S gate (Bech-Otschir et al., 2009; Li and Demartino, 2009). The binding of polyubiquitin to the Usp14/Ubp6 subunit of the 19S particle appears crucial, as this triggers gate opening, leading to translocation of the target protein into the core and subsequent proteolysis (Peth et al., 2009). Further work, especially a high resolution structure of the 19S particle, is necessary for complete understanding of this complex machine.

Proteolysis can only be an effective form of regulation if there is specificity about which proteins are degraded at which times. The specificity in the ubiquitin-proteasome system comes from E3 ligases, of which there are two major types in eukaryotes: HECT domain-containing and RING domain-containing. HECT (homologous to E6-AP C-terminus) domain E3s possess

catalytic activity in that the ubiquitin moiety is covalently attached to the E3 from the E2, and this monomer is then passed to the substrate. The HECT domain is the site of interaction with the E2 and consists of ~350 amino acids, including the cysteine which receives the ubiquitin monomer (Scheffner and Staub, 2007). 28 HECT domain-containing genes occur in the human genome, including E6-AP (human papilloma virus E6-associated protein), Nedd4, and the TGF/BMP regulators Smurf1 and Smurf2.

The majority of E3s are of the RING (really interesting new gene) domain type, with at least 300 occurring in the human genome (Deshaies and Joazeiro, 2009). The RING domain is made up of cysteines and histidines spaced with other amino acids in an orientation that coordinates two zinc ions within the protein, and it is through this domain that E2s are recruited. Among RING E3s, two classes exist: those in which the RING domain and substrate-binding domain are in the same protein, and those in which a generic RING domain protein serves as a subunit in a complex with other proteins, including a substrate-binding protein. Of the latter type, the most common are SCF complexes, in which an Rbx/Roc protein provides the RING domain for E2 binding, a cullin protein serves as a scaffold to bind the RING domain protein and a SKP1-related protein. The substrate specificity in the SCF complex comes from the F box protein, which binds to SKP1 via its F box domain and the substrate through its substrate specificity site, bringing the substrate in proximity with the E2 and catalyzing ubiquitin conjugation.

The F box is named for cyclin F, the first protein recognized with this domain (Kraus et al., 1994), but the first SCF complex described consists of *Saccharomyces cerevisiae* Cdc4 as the F box protein along with Cul1 and Skp1, an E3 complex that degrades Sic1 and other proteins (Feldman et al., 1997). The interaction between Cdc4 and Sic1 requires phosphorylation of Sic1, underlining a common theme among F box-substrate interactions in which the substrate must be somehow modified to improve the protein-protein interaction (Hao et al., 2007). In another example, N-glycan modification is required to induce interaction of the SCF^{Fbx2} ubiquitin ligase complex with its substrates in the ER-associated degradation (ERAD) pathway (Yoshida et al., 2002).

Despite the inordinately large number of F box proteins in the *C. elegans* genome (at least 200), few have been assigned functions or SCF partners. One complicating factor is that, instead of one human SKP1, there are 21 *C. elegans skr-* (*SKP1-related-*) genes. Of these, *skr-1* and *-2* are most closely related to human SKP1, as well as being adjacent in the *C. elegans* genome and 83% identical (Nayak et al., 2002; Yamanaka et al., 2002). Injection of RNAi against *skr-1* or *-2* into the gonad of hermaphrodites led to the embryonic lethality of their progeny, due to cellular hyperplasia, a phenotype similar to *cul-1* and *lin-23* mutants. Because of the similarity between *skr-1* and *-2*, it is unlikely that the RNAi is specific to either gene, making it impossible to determine which gene, or both, is responsible for this phenotype. However, several lines of evidence suggest that *skr-1* alone is relevant. First, Yamanaka et al. report that *skr-1* is

expressed ubiquitously from gastrulation to adulthood, while *skr-2* is restricted to the gut (Yamanaka et al., 2002). Second, Killian et al. report isolation of a deletion allele, *tm2391*, which deletes *skr-1* but not *skr-2* (Killian et al., 2008). This allele is embryonic lethal, with rare escapers displaying the SCF^{lin-23} hyperplasia phenotype. Finally, a hypomorphic missense allele of *skr-1*, *sm151*, fails to complement *tm2391*, giving further credence to the idea that *tm2391* affects only *skr-1* (Killian et al., 2008).

While the ubiquitin-proteasome system has a role in virtually every process in cell biology, it is especially important for the regulation of apoptosis. The IAP (inhibitor of apoptosis) proteins, for example, are E3 ligases which are crucial for cell death control in vertebrates and *Drosophila*. IAPs contain between one and three BIR (baculovirus IAP repeat) domains which are required for binding to caspases, as well as a C-terminal RING domain, through which IAPs mediate E2 recruitment. The *Drosophila* protein DIAP1 acts as an inhibitor for caspases to keep them in check; DIAP1 mutants die during embryogenesis due to excessive cell death (Goyal et al., 2000; Lisi et al., 2000; Wang et al., 1999; Wilson et al., 2002). In addition to BIR and RING domains, DIAP1 contains an IAP binding motif (IBM) which mediates its interaction with upstream IAP antagonists such as Reaper, Hid and Grim. These pro-apoptotic molecules promote DIAP1 auto-ubiquitination and destruction by the proteasome with the help of UBCD1, inducing apoptosis (Ryoo et al., 2002; Wilson et al., 2002). DIAP1 is also controlled by N-end rule ubiquitination, but the physiologic role of

this modification remains an open question, as it has been reported to be both pro-apoptotic (Yokokura et al., 2004) and anti-apoptotic (Ditzel et al., 2003).

These results suggest that a pro-apoptotic protein like Reaper binds to DIAP1 to induce its auto-ubiquitination and degradation, releasing caspases from BIR domain binding and causing apoptosis. However, deletion of the RING domain increases rather than decreases apoptosis suggesting that DIAP1 also contains anti-apoptotic function. DIAP1 polyubiquitinates the caspases DRONC and drICE, inhibiting their activation either through a non-degradative pathway (Chai et al., 2003; Ditzel et al., 2008; Lisi et al., 2000; Ryoo et al., 2002; Ryoo et al., 2004; Wilson et al., 2002). When DRONC is associated with Dark in the context of the apoptosome, however, DIAP1 appears to ubiquitinate it and induce its degradation (Shapiro et al., 2008). Thus, the DIAP1 ubiquitin ligase is a complicated and central regulator of *Drosophila* apoptosis.

In mammals, the E3 ligase XIAP prevents apoptosis when overexpressed and inhibits caspases-3, -7 and -9. While the RING domain is not required for this inhibition *in vitro* (Deveraux et al., 1997), *in vivo* deletion of the RING results in mice predisposed to cancer and susceptible to pro-apoptotic insults (Schile et al., 2008). This inhibition is the result of polyubiquitination of caspase-3 without accompanied degradation, suggesting that XIAP acts as an E3 for its function, not a simple caspase-binding inhibitor. Another mammalian ubiquitin ligase complex implicated in apoptotic regulation is Bruce/Apollon, an E3 for caspase-9 and Smac/Diablo (Bartke et al., 2004; Hao et al., 2004).

Ubiquitin modification is not only important for caspase control in apoptosis, but also in regulating caspase activation in non-death related contexts. One example is in the process of *Drosophila* sperm individualization, in which spermatids remove the bulk of their cytoplasm and organelles in a process that requires caspases but does not kill the cells (Arama et al., 2003). By screening through a collection of male-sterile genetic mutants for defects in active caspase staining, a cullin3-based E3 ligase complex made up of $Cul3_{Testis}$, Roc1b, and Klhl10 are required for caspase activation and sperm individualization. dBruce, a giant BIR and UBC domain-containing protein that is also required for sperm viability, interacts with the substrate-specificity domain of Klhl10 and may be the relevant target for this E3 ligase (Arama et al., 2007). The same screen yielded another mutant, *ms771*, which maps to a gene containing an F box, *nutcracker*. Nutcracker functions in an SCF complex with Cullin-1 and SkpA to regulate caspase activation in a unique way: it regulates the activity of proteasomes in the developing spermatid. While there is no change in proteasome number in the nutcracker mutant, protein extracts from nutracker mutant testes showed a reduced ability to degrade a fluorogenic probe, suggesting a role for *nutcracker* in stimulating proteasome function (Bader et al., 2010).

In addition to direct regulation of apoptosis via caspases, the ubiquitin-proteasome system has also been implicated in control of BCL2-family members. For example, Bim was reported to be ubiquitinated and degraded following ERK1/2 phosphorylation (Akiyama et al., 2003; Ley et al., 2003). The Bid protein

must be cleaved to become active, as its N-terminal fragment obscures the pro-apoptotic BH3 domain, located in the C-terminal fragment. After cleavage, the N-terminal inhibitory fragment is ubiquitinated and degraded, and this ubiquitination is unusual in that it occurs not on lysines but on serines, cysteines and threonines (Tait et al., 2007). Zhong et al. reported that a HECT E3 ligase, HUWE, can bind to and polyubiquitinate MCL-1, an anti-apoptotic BCL2-like protein, and that HUWE contains a domain similar to the BH3 domain which promotes binding to MCL-1 (Zhong et al., 2005). Finally, BCL2 has been reported to be degraded by the proteasome, as well as phosphorylated to regulate its activity. Dimmeler et al. showed that human endothelial cells treated with TNF-α degrade endogenous BCL2, and that this degradation can be inhibited by mutating lysines in the protein. In this system, dephosphorylation increased BCL2 degradation, possibly through a MAP kinase module (Breitschopf et al., 2000; Dimmeler et al., 1999). Phosphorylation of BCL2 was also reported to induce its proteasomal degradation, as is commonly the case with F box protein substrates. The relevant E3 has not been identified, but Lin et al. reported that the phosphatase PP2A dephosphorylates BCL2 to prevent its degradation and that reduction of PP2A activity led to BCL2 phosphorylation and degradation (Lin et al., 2006).

DRE-1, a conserved F box protein

The mammalian homolog of dre-1, FBXO11, was first named VIT1, as its partial cDNA was isolated from melanocytes from patients with vitiligo (Le Poole et al., 2001). In these cells, FBXO11 was expressed at lower levels than in control melanocytes. An in silico approach was used to identify a putative protein arginine methyltransferase (PRMT) domain in the protein, although this domain is divergent from other PRMT proteins (Cook et al., 2006). An *in vitro* methylation assay using immunoprecipitated PRMT9 isoform 4 (which lacks the F box) from HeLa cells, showed the capacity to methylate various histone and synthetic peptide substrates. Abida et al. reported that FBXO11 can interact with p53 and induce its neddylation, and that this modification inhibits p53 transcriptional activity (Abida et al., 2007).

In developing mice, Fbxo11 protein was detected by immunohistochemistry starting at embryonic day 9.5, when staining was confined to the developing heart. Later in development, expression was detected in liver, muscle, palatal epithelia, lung, kidney, adrenal gland, bone marrow, skin, hematopoietic cells, osteoblasts, spleen and middle ear. In adults, of the tissues studied, staining occurred in alveolar macrophages, glomeruli and collecting tubules in the kidney, midbrain, heart and muscle (Hardisty-Hughes et al., 2006).

Two mutant mouse lines exist with lesions in mouse Fbxo11. The Jeff mouse was isolated from an ENU screen for deafness and exhibits worsening deafness over time as a heterozygote, possibly due to chronic otitis media

(Hardisty et al., 2003). Heterozygotes are 21% smaller than their wild-type littermates and have a mild craniofacial abnormality. As homozygotes, all Jf/Jf animals died at birth or within a few hours because of respiratory difficulty and had upper eyelids open. In addition, the craniofacial abnormalities were more severe, with facial clefting and clefting of the soft or hard palate. A second mouse, Mutt, also contains a mutation in Fbxo11, and partially recapitulates the Jeff deafness, craniofacial abnormality and perinatal lethality phenotypes, but lacks otitis media and is likely a milder hypomorphic allele (Hardisty-Hughes et al., 2006).

Further studies by the same group focused on TGF-β pathway proteins in the Jeff mouse because the palatal and eyes-open-at-birth (EOB) phenotypes have been observed in mutants in this pathway such as TGF-β-3, though not all mutants with these phenotypes are TGF-β-related (for example, Apaf-1 null mice have similar craniofacial and palatal fusion defects). Tateossian et al. showed no effect of Fbxo11 mutation on expression of Fbxo11, TGF-β-3, TGF-βRI or Smad 4, but an increase in nuclear phospho-Smad2 in developing palates of Fbxo11 homozygotes at E15.5 as assayed by immunohistochemistry, compared to wild-type. While there were no differences in proliferation as measured by Ki67 staining in wild-type vs. Jeff palates, there was a modest but statistically significant reduction in the number of cells stained with an anti-cleaved caspase-3 antibody (Tateossian et al., 2009).

Characterization of the eyelid phenotype of Fbxo11 homozygotes showed a similar pattern of staining: no differences were observed in expression of Fbxo11, TGF-β-3, TGF-βRI or Smad 4, but an increase in nuclear phospho-Smad2 was seen at day 15.5. Again, no differences were evident in Ki67 staining, but there was a significant reduction in the level of cleaved caspase-3 in Fbxo11 homozygotes. Smad2/+; Fbxo11/+ animals showed a significant lethality defect (66% died soon after birth), as well as respiratory difficulty. Immunoprecipitation of Fbxo11 failed to detect an interaction with Smad2 or p53 (Tateossian et al., 2009).

Chapter 2: Genetic control of tail-spike cell fusion and tail morphogenesis

2.1 Background

As reported by Sulston, the tail-spike cell is born as two precursor cells, the sisters of the hyp10 precursors, which fuse during embryogenesis to form a single syncitium, differentiate by extending a thin microtubule-containing process posteriorly, and die during late embryogenesis (Fig. 3).

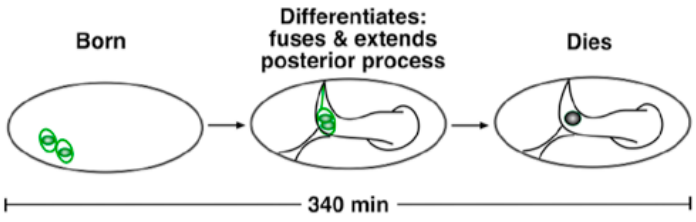

Fig. 3. The life and death of the tail-spike cell.
The tail-spike cell lives for ~340 minutes, and during that time undergoes fusion and differentiation. Reproduced from (Maurer et al., 2007).

In *C. elegans*, 300 out of 959 nuclei of the somatic cells are parts of syncitia. In addition, because of the stereotyped nature of *C. elegans* development, the cells which fuse have the same partners and fuse predictably. Two genes have been isolated from screens for defective fusion, *eff-1* and *aff-1*, which are conserved in other nematodes but do not have homologues in other organisms. *eff-1* was isolated from a screen in which animals expressing an adherens junction protein labeled with GFP (AJM-1::GFP) failed to fuse cells that normally fuse. *eff-1* mutants fail to fuse all 43 epidermal cells that are programmed to fuse during embryogenesis, and also show defects in fusions post-embryonically (Mohler et al., 2002). Mohler et al. reported that *eff-1* mutants have abnormalities in tail-spike morphogenesis, as well as misshapen male tails in which the tail-spike persists inappropriately. It was later shown that *eff-1* is required in both fusing cells to induce fusion, and that expression of *eff-1* was sufficient to induce fusion of heterologous insect cells (Podbilewicz et al., 2006).

While the majority of fusions require *eff-1*, certain cells remain competent to fuse in *eff-1* mutants, including the anchor cell, which fuses during normal vulval development to open the vulva for egg-laying. Sapir et al. screened for egg-laying defective animals and examined anchor cell fusion to identify a mutation in the *aff-1* gene (*anchor cell fusion failure-1*) (Sapir et al., 2007). *aff-1* is structurally similar to *eff-1*, and, like *eff-1*, can induce fusion when expressed ectopically in *C. elegans* as well as when expressed in heterologous cells.

While the work described above defined the genes necessary for many fusions in *C. elegans* development, the gene(s) required for tail-spike cell fusion were not known. In addition, the role of fusion in regulation of cell death has not been investigated.

2.2 Results

aff-1 is required for tail-spike cell fusion

We wondered whether fusion played a role in tail-spike cell death. To address this question, we first tested whether *aff-1* (*anchor cell fusion failure-1*), a newly-described fusogen that is required for fusion of the anchor cell during vulval development as well as for the fusions of a number of other cell pairs, was required for tail-spike cell fusion. A previously-isolated fusogen, *eff-1* (*epithelial fusion failure-1*) was found by Carine Maurer to have no role in tail-spike cell fusion (Maurer, PhD thesis). *aff-1*, however, was required for tail-spike cell fusion, as we observed two healthy but unfused cells in *aff(tm2214);ced-3(n717);nsIs25* animals. We conclude that *aff-1*, but not *eff-1*, is required for tail-spike cell fusion.

For further evidence that *aff-1* is involved in tail-spike cell fusion, we tested whether a transcriptional reporter for *aff-1* was expressed in the tail-spike cell. Indeed, the 4.5 kb genomic fragment upstream of the *aff-1* start codon drove GFP expression within the tail-spike cell in *ced-3(n717)* animals (Fig. 4). GFP

was also expressed in other cells throughout the animal, but, importantly, not in hyp10.

Fig. 4. *aff-1pro::gfp* is expressed in the tail-spike cell.
Fluorescence images of tails of two representative L1 *ced-3(n717)* animals in which GFP expression is evident in the tail-spike cell.

Having established *aff-1* as the relevant fusogen for the tail-spike cell, we could address whether fusion was required for death. In *aff-1(tm2214);nsIs25* animals, 0% of L1s had surviving tail-spike cells, showing that unfused cells are fully capable of undergoing programmed cell death.

Tail-spike cell non-fusion affects tail morphogenesis

While examining *aff-1(tm2214)* mutants, we noticed an unusual tail morphology defect: a large number of L1s had forked tails. Quantification of this serendipitous finding showed that 78% of *aff-1(tm2214)* L1s had forked tails, while 0% of N2 L1s and 0% of *eff-1(hy40)* L1s had forked tails (*eff-1* animals frequently had rounded tail tips or tail tips with knobs attached) (Fig. 5). The percentage of animals with forked tails in *aff-1(tm2214)* may be an underestimate because we observed some animals in which one fork was significantly smaller or broken, suggesting that the fork may not always be even and the smaller half may be lost during the animal's life.

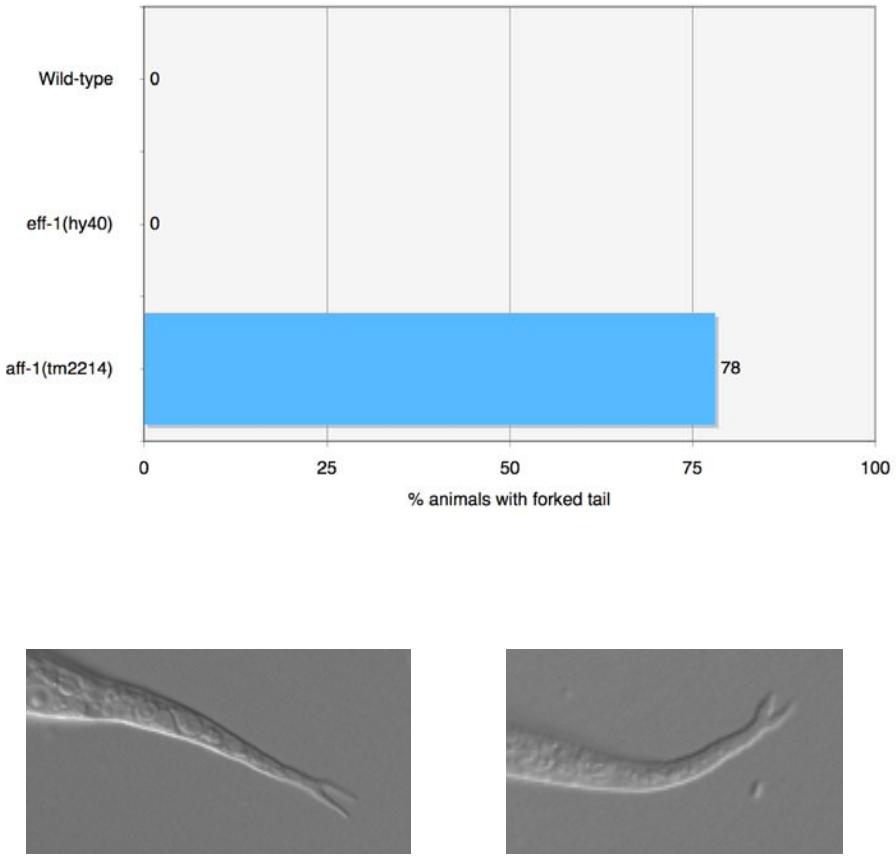

Fig. 5. *aff-1(tm2214)* but not *eff-1(hy40)* or wild-type animals have forked tail-tips.
Top: Quantification of the percentage of animals with forked tails, as assessed by DIC microscopy (n>100 for each genotype).
Bottom: Representative images from two L1 *aff-1(tm2214)* animals, showing the forked tail defect common in this mutant.

Given that Sulston had postulated that the tail-spike cell process forms a scaffold for hyp10 morphogenesis, and given the electron microscopic (EM) results showing a microtubule core within the tail-spike cell that persists after its death, we wondered whether the *aff-1(tm2214)* forked tail phenotype might be related to the tail-spike cells remaining unfused. In examining *aff-1(tm2214);ced-3(n717);nsIs25* animals more carefully, we were able to identify many animals in which each unfused tail-spike cell had generated a process extending into the posterior of the animal. Thus, it is likely that, with two microtubule-containing processes within itself instead of one, hyp10 is improperly patterned in *aff-1(tm2214)* animals, and the forked tail phenotype results. While these results are not proof that the tail-spike cell fusion defect is responsible for the forked tail phenotype (a tail-spike cell-specific rescue of the *aff-1* mutation would be necessary to prove this, an experiment that is rendered impossible because we lack an early tail-spike cell-specific promoter), the correlation between two processes and forked tails is striking evidence to support this idea.

2.3 Conclusion

These results lend support to the Sulston model in which the tail-spike cell's major, or possibly sole, function is to extend a microtubule-laden process posteriorly during embryogenesis to direct proper hyp10 morphogenesis and tail-tip shape. Presumably, when this function has been served, the cell is no longer necessary for the organism, and thus undergoes programmed cell death. In the

context of failed tail-spike cell fusion as in *aff-1* mutants, each unfused tail-spike cell appears able to direct morphogenesis of a separate tail-spike, leading to a forked tail. Thus, proper tail-spike cell morphogenesis in the form of a fused cell with one process is crucial to building the elegant *C. elegans* tail-spike.

Chapter 3: Cloning and characterization of a novel regulator of programmed cell death

3.1 Background

The tail-spike cell as a system for uncovering apoptotic regulators

A great many screens have been performed to find regulators of apoptosis, and these screens have defined the core apoptotic machinery to include *egl-1*, *ced-9*, *ced-4* and *ced-3* in a linear pathway.

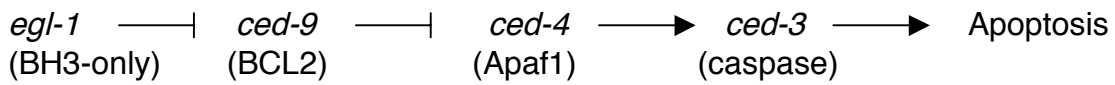

With these screens for global cell death genes saturated, we turned to studying individual cells as a way to better understand the mechanisms of apoptosis. Of the individual cells that undergo programmed cell death in *C. elegans*, we chose to study the tail-spike cell for two major reasons. First, the tail-spike cell is one of only a few cells that is long-lived during *C. elegans* development before undergoing apoptosis. While most cells die within 20 minutes of being born, the

tail-spike cell lives 10 times as long, and during that time differentiates by extending a process posteriorly. Thus, it more closely resembles the deaths of mammalian cells, which die after differentiation. Second, and most importantly, the genetic control of tail-spike cell death is unique. While *egl-1* is required for virtually all other deaths in the worm, in the tail-spike cell it is dispensable for death. Worms carrying a non-functional *egl-1* gene have a persistent tail-spike cell 30% of the time. In other words, in 70% of animals, the tail-spike cell can be specified for death and execute that fate in the complete absence of *egl-1* activity (Fig. 6). With *ced-3* and *ced-4* being completely required for tail-spike cell death, we recognized that the tail-spike cell represents an ideal system for uncovering new regulators of caspase activation: in the absence of *egl-1*, some other gene(s) must be responsible for activating *ced-3* and *ced-4*. We set out to identify these gene(s).

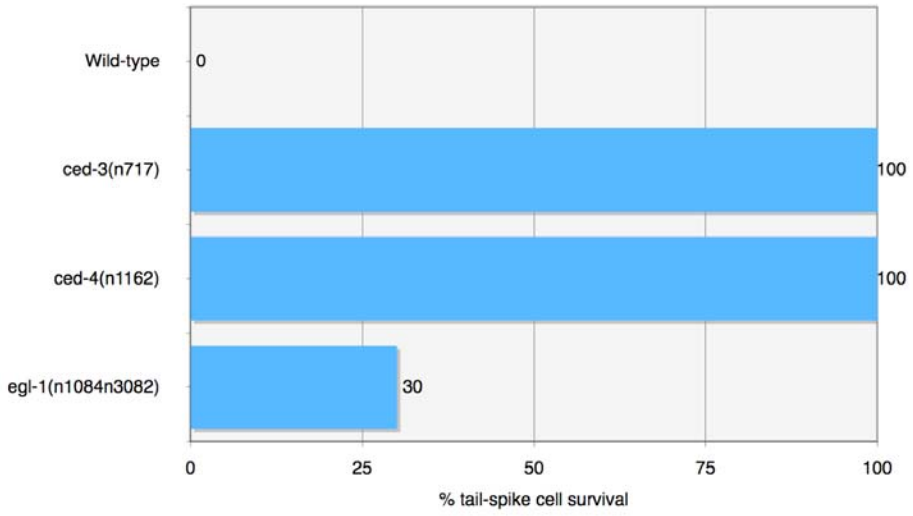

Fig. 6. Tail-spike cell death requires *ced-3* and *ced-4* but *egl-1* is dispensable for death.
Percentage of animals with a surviving tail-spike cell in *ced-3(n717)*, *ced-4(n1162)* and *egl-1(n1084n3082)* strains. All strains contain the *nsIs25* transgene to mark the tail-spike cell (n>100 for each). Reproduced from (Maurer et al., 2007).

3.2 Results

A forward genetic screen for regulators of tail-spike cell death

To identify the gene(s) acting in place of *egl-1* in the tail-spike cell to regulate apoptosis, Carine Maurer performed a forward genetic screen on animals carrying the *ced-3pro::gfp* integrated transgene (*nsIs25*) which marks the tail-spike cell. She mutagenized *nsIs25* animals with ethyl methanesulfonate, screened the F2 progeny for animals with surviving tail-spike cells and isolated 8 putative mutants, *ns16*, *ns17*, *ns18*, *ns19*, *ns38*, *ns39*, *ns40* and *ns41*. In addition to looking for animals in which the tail-spike cell survived, she focused on mutants that lacked a global cell death defect as a way to avoid alleles of *ced-3* and *ced-4*. We checked these 8 mutants for survival of the tail-spike cell: 5/8 had <1% tail-spike cell survival, and because of the low penetrance of the defect, chose not to pursue these mutants (Fig. 7). Of the remaining 3, *ns38* had a significant global cell death defect (7.2 extra cells in the pharynx, as assayed by Shai Shaham), and *ced-3* failed to complement this defect. We conclude that *ns38* is an allele of *ced-3*. The remaining two mutants, *ns39* and *ns40*, fail to complement each other, and thus likely represent lesions in distinct genes. 19% of *ns40;nsIs25* animals have a surviving tail-spike cell.

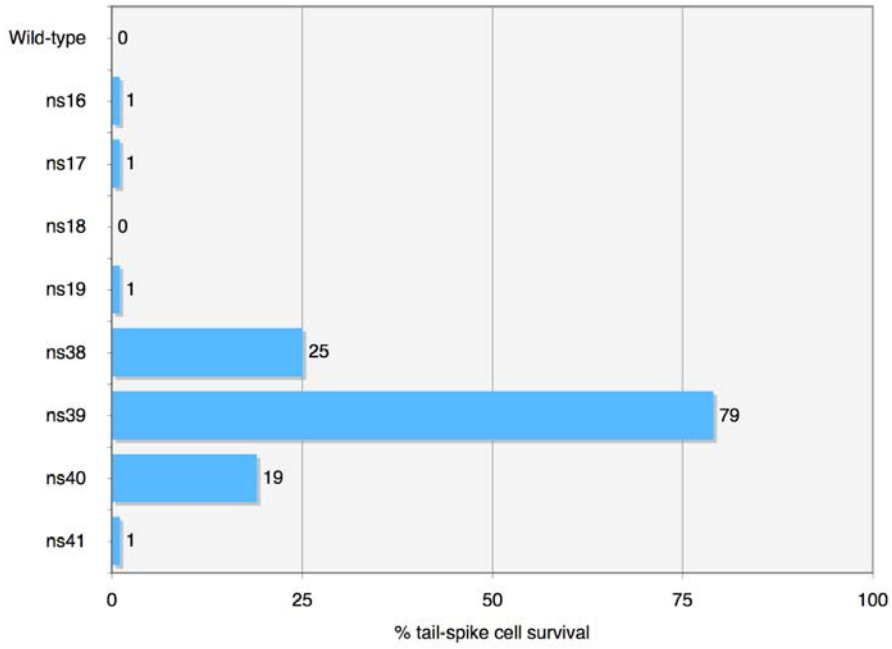

Fig. 7. Tail-spike survival in mutants isolated from a forward genetic screen.

Percentage of animals with a surviving tail-spike cell in strains with the indicated genotypes. *ns16*, *ns17*, *ns18* and *ns19* contain the *nsIs23* transgene while *ns38*, *ns39*, *ns40* and *ns41* contain the *nsIs25* transgene to mark the tail-spike cell (n>100 for each).

The tail-spike cell survives inappropriately in ~79% of animals carrying the *ns39* mutation, compared to 0% in wild-type animals. In addition, the surviving tail-spike cell in *ns39;nsIs25* animals expresses *ced-3pro::gfp*, indicating that *ced-3* transcription is intact and placing *ns39* in a different class from *pal-1*-like mutants in which tail-spike cell death is prevented by lack of *ced-3* transcription. In *ns39* mutants the tail-spike precursor cells fuse properly and the cell extends a process posteriorly, making the surviving tail-spike cells in this strain indistinguishable from those in *ced-3* or *ced-4* mutant strains.

The result that the tail-spike cell survives inappropriately in 79% of animals implies that it is born and dies appropriately in the remaining animals. To test this assumption, I crossed the *ns39* mutation to the *ced-5(n1812)* background, in which apoptotic corpses are not engulfed, making their identification by DIC microscopy easy. In this background, the tail-spike cell survived 71% of the time and in all of these animals no corpse was evident in the tail (Fig. 8). In 29% of animals, a corpse was present in the proper position that harbored residual GFP expression, and no other cells in the area expressed GFP. Finally, there were zero animals in which neither a surviving cell nor a corpse were present, or both were present. Thus, the reason for no tail-spike cell being evident in *ns39;nsIs25* animals is that it has died, not that it was never generated, or that it was alive but the *ced-3pro::gfp* marker had not been activated.

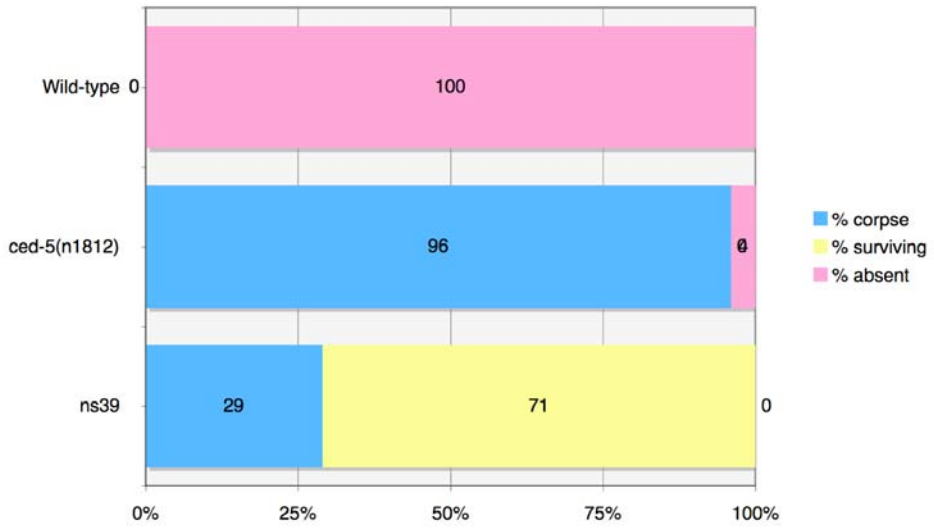

Fig. 8. The *ns39* mutation blocks tail-spike cell death but does not alter cell fate.
The status in L1 animals of the tail-spike cell was assessed in wild-type, *ced-5(n1812)* engulfment defective, and *ns39; ced-5(n1812)* backgrounds. In wild-type animals, the cell always dies and the corpse is cleared. In *ced-5(n1812)* animals, the cell always dies and the corpse is evident in 96% of animals. In *ns39; ced-5(n1812)* animals, the cell survives in 71% of animals and can be seen as a healthy cell; in the remaining 29% of animals, the cell dies and its corpse can be identified (n>100 for each).

Because these observations about the *ns39* mutation are consistent with it blocking *ced-3* caspase activation in the tail-spike cell to prevent apoptosis, I decided to pursue this mutant further.

The *ns39* mutation maps to the *dre-1* gene

After backcrossing five times, I used standard SNP-mapping techniques to map the *ns39* mutation to a region on Chromosome V between -0.183 and 0.109 MU. Within this region, several genes were reported to have an egg-laying defect, as was observed in the *ns39* strain. Of these, I sequenced the *dre-1* (*daf-12-redundant-1*) gene and identified a C to T change, consistent with this being an EMS-induced mutation. This lesion is predicted to induce a serine to leucine missense mutation at position 275 of the protein (based on the "new" cDNA, see below).

dre-1 was named by Adam Antebi's group who were studying the effects of *daf-12* on developmental timing. They isolated several alleles of *dre-1*, including *dh99* and *dh279*. I tested whether these alleles shared the tail-spike cell death phenotype of *ns39* by crossing them to the *nsIs25* marker. Indeed, both of these independently isolated alleles showed tail-spike cell death defects, of 12 and 2%, respectively, consistent with *dre-1* being the gene responsible for the *ns39* defect (Fig. 9).

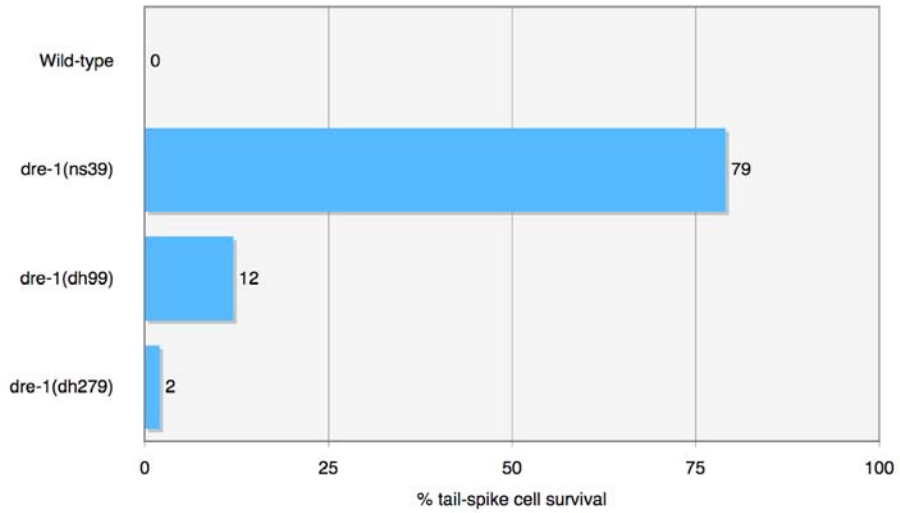

Fig. 9. Mutations in *dre-1* block tail-spike cell death.
Percent of animals with a surviving tail-spike cell in strains with the indicated genotypes (n>100 for each). All strains contain the *nsIs25* transgene to mark the tail-spike cell.

To further demonstrate that *dre-1* is the relevant gene for tail-spike cell death, I did a complementation test between two independently isolate alleles of *dre-1* – *ns39* and *dh99*. 25% of animals with the genotype *ns39/dh99* had a surviving tail-spike cell, showing that *ns39* and *dh99* fail to complement each other and lending further support to the idea that *dre-1* controls tail-spike cell death (note that this percentage may be an underestimate of tail-spike cell survival in these animals as the *nsIs25* marker was heterozygous in all animals scored) (Fig. 10). In the course of this cross, I also generated animals heterozygous for either *ns39* or *dh99*; none of these animals had a surviving tail-spike cell, demonstrating that both mutations are recessive with respect to tail-spike cell death. In addition, I found that *ns39*/*gk857* animals (*gk857* is a deletion that removes 599 bp of the *dre-1* cDNA from position 155 to 753) are mostly inviable. The few animals of this genotype I was able to produce died as L1 larvae (5 animals). None of these animals had a surviving tail-spike cell, though they were very sick and died soon afterwards.

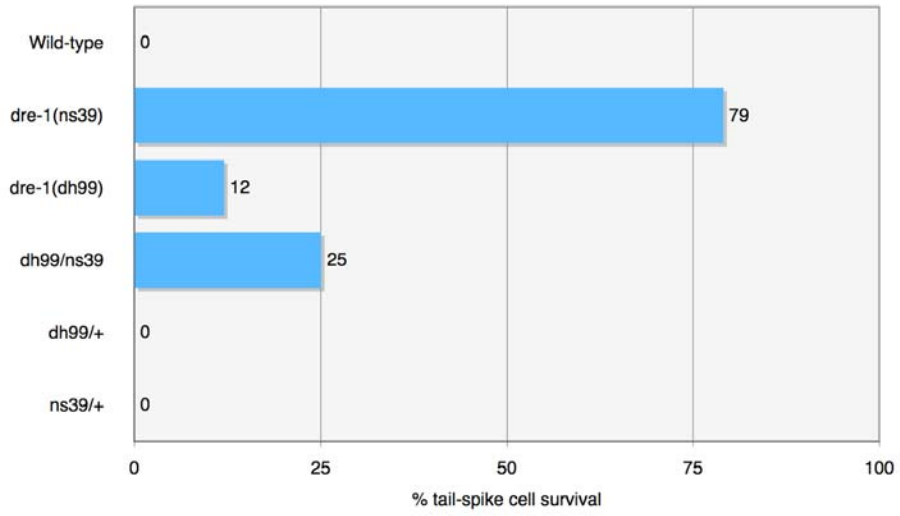

Fig. 10. *dre-1(dh99)* and *dre-1(ns39)* fail to complement each other with respect to the tail-spike cell death defect.
Percent of animals with a surviving tail-spike cell in strains with the indicated genotypes (n>100 for each). All strains contain the *nsIs25* transgene to mark the tail-spike cell.

If *dre-1* is involved in promoting tail-spike cell death, then ectopically expressing wild-type *dre-1* in the tail-spike cell of *ns39* mutants should induce apoptosis. I used several methods to rescue the *ns39* phenotype.

First, I injected two overlapping fosmids that include the *dre-1* sequence into the *ns39* mutant. WRM067bH07 contains 31.7 kb of genomic sequence, including 13.5 kb upstream of the "old" dre-1 ATG (see below) and 13.8 kb downstream of the stop codon. This fosmid rescued the tail-spike cell death defect fully, giving 2% survival in transgenic animals (Fig. 11). WRM0637aG11 contains 33.7 kb of genomic sequence, including 21.1 kb upstream of the "old" dre-1 ATG (see below) and 8.2 kb downstream of the stop codon. This fosmid also rescued the tail-spike cell death defect, giving 7 and 13% survival in two independent lines. Thus, the information required for rescue is contained within these ~30 kb of genomic sequence.

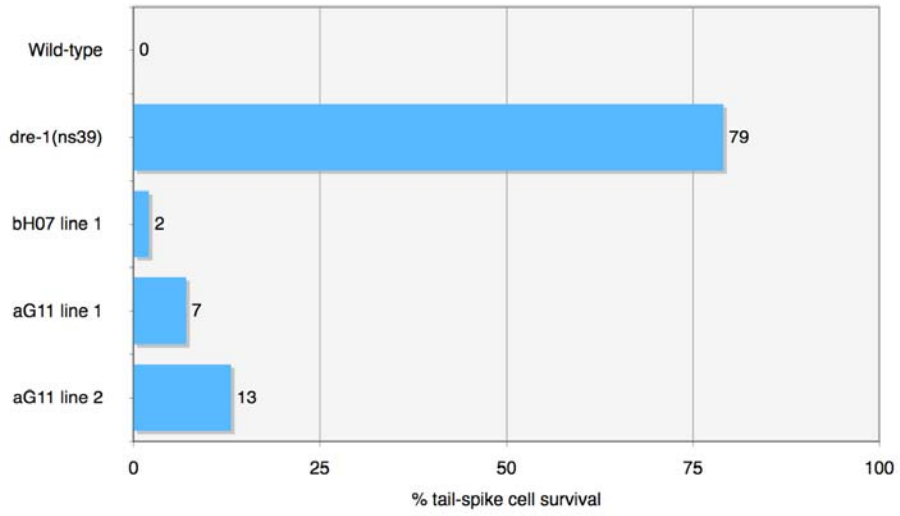

Fig. 11. Two fosmids containing the *dre-1* locus rescue the tail-spike cell death defect in *dre-1(ns39)* animals.
Percent of animals with a surviving tail-spike cell in wild-type, *dre-1(ns39)*, and *dre-1(ns39)* + indicated fosmid (n>100 for each). All strains contain the *nsIs25* transgene to mark the tail-spike cell.

The overlapping region within these two fosmids contains *dre-1*, *acs-1* (*fatty acid CoA synthetase-1*), *F46E10.11* (a predicted non-coding RNA), and *twk-10* (a potassium channel). To determine whether *dre-1* is in fact the relevant gene, I attempted to rescue the *ns39* phenotype with the *dre-1* cDNA. Initial attempts to rescue using the cDNA reported by Adam Antebi's group (Fielenbach et al.) driven by 4.4 kb of genomic sequence upstream of the ATG failed to rescue, and Fielenbach et al. reported difficulty in rescuing with the cDNA and instead only rescued with a YAC and a 15 kb genomic fragment.

We wondered whether the reported cDNA was incomplete. Examination of the sequence upstream of the ATG identified a putative splice donor site ~8kb upstream. In addition, Aceview.org reported an incomplete cDNA clone using this ATG spliced to the reported sequence that is in frame. To test whether this putative exon was in fact part of the *dre-1* cDNA I performed PCR on cDNA isolated from mixed stage worms graciously provided by Maya Tevlin. A forward primer beginning with the "new" ATG and a reverse primer in the "old" first exon produced a band of the proper size if this "new" exon was in fact spliced to the "old" cDNA (Fig. 12). Sequencing of this product revealed an in-frame splice junction. In addition, PCR using a forward primer corresponding to the SL1 splice leader sequence and a reverse primer within the "new" first exon produced a product that was the expected length and sequence, showing that this ATG is in fact utilized in the worm and that it is SL1 spliced. In addition, SL1 splicing occurs to the "old" dre-1 cDNA, as previously reported (Fielenbach et al.) but it is

unclear whether this transcript is in fact biologically relevant.

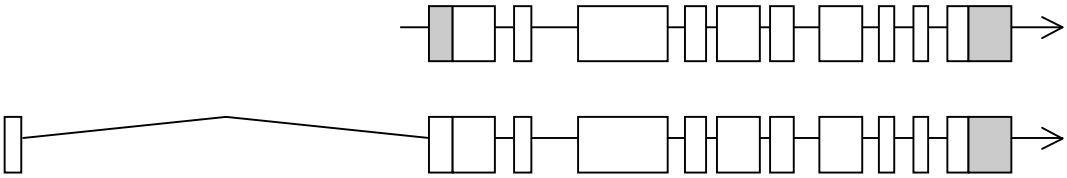

Fig. 12. Exon structure of the "old" versus "new" *dre-1* cDNA.
The new cDNA (bottom) includes an exon 8 kb upstream of the originally reported start codon. SL1 splicing was detected in both forms.

The new cDNA is 258 bp longer, and converts the 5'UTR from the old cDNA into coding sequence, producing a protein that is 86 amino acids longer. This sequence is conserved in *C. briggsae*, though it yields no new domains and is not conserved in other organisms.

Using this new dre-1 cDNA in rescue experiments proved successful. A construct consisting of the new dre-1 cDNA under the *aff-1* promoter and including the *dre-1* 3'UTR rescued the *dre-1(ns39)* tail-spike cell death defect. In 3 independent lines, tail-spike cell survival was reduced from 79% to 11, 22 and 46% (Fig. 13). This experiment warrants two conclusions. First, this shows that loss of *dre-1* is responsible for the *ns39* phenotype and establishes *dre-1* as a regulator of apoptosis in the tail-spike cell. Second, because the *aff-1* promoter expresses in the tail-spike cell but not its sister, hyp10, this experiment shows that *dre-1* acts cell autonomously to induce tail-spike cell death.

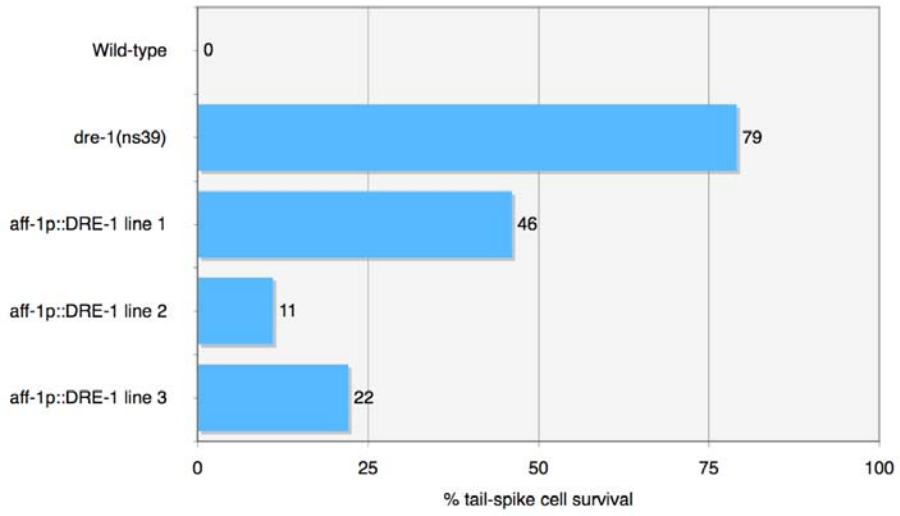

Fig. 13. Expression of the DRE-1 cDNA under the *aff-1* promoter rescues the *dre-1(ns39)* tail-spike cell death defect.
Percent of animals with a surviving tail-spike cell in wild-type, *dre-1(ns39)*, and *dre-1(ns39)* + *aff-1p*::DRE-1 transgenes (n>100 for each). The *aff-1* promoter expresses in the tail-spike cell but not hyp10. All strains contain the *nsIs25* transgene to mark the tail-spike cell.

In addition, we also expressed the *dre-1* cDNA under the *dpy-30* ubiquitous promoter (Fig. 14). This construct also rescued the *dre-1(ns39)* defect, albeit less well, possibly because this promoter is not very strong (Shai Shaham, personal communication).

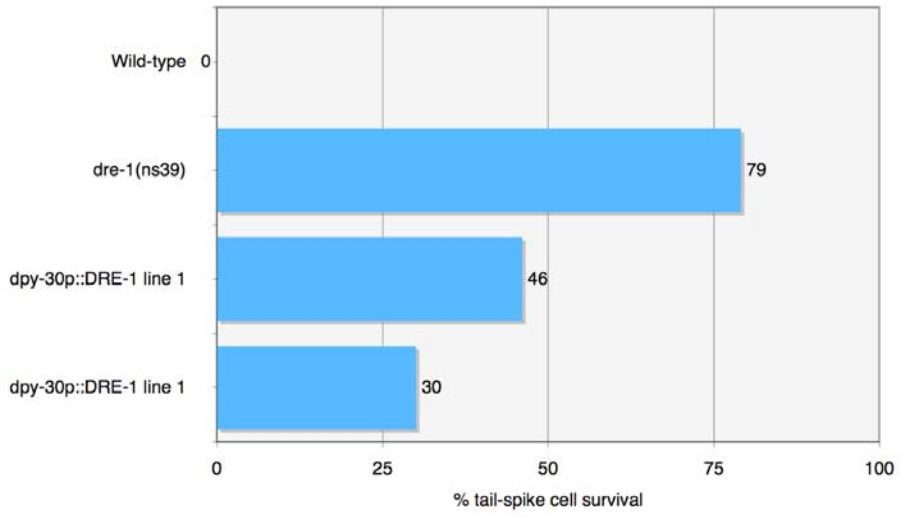

Fig. 14. Expression of the DRE-1 cDNA under the *dpy-30* ubiquitous promoter rescues the *dre-1(ns39)* tail-spike cell death defect.
Percent of animals with a surviving tail-spike cell in wild-type, *dre-1(ns39)*, and *dre-1(ns39)* + *dpy-30p*::DRE-1 transgenes (n>100 for each). All strains contain the *nsIs25* transgene to mark the tail-spike cell.

Having established that *dre-1* is required cell autonomously for tail-spike cell death, I investigated its expression pattern. Fielenbach et al. had described *dre-1* as being expressed in many cells during embryogenesis, especially epidermal-like cells (Fielenbach et al., 2007). A 4 kb promoter construct taken from intron 1 of the dre-1 gene expressed in many cells, including the tail-spike cell (Fig. 15). The tail-spike cell expression was confirmed by co-expressing RFP under the control of the *ced-3* promoter which marks the tail-spike cell. Thus, *dre-1* is expressed and acts in the tail-spike cell to control death.

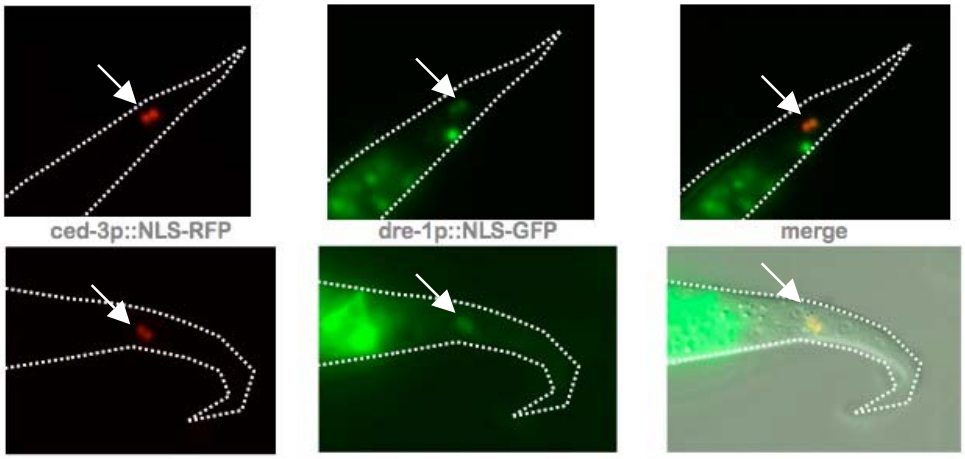

Fig. 15. *dre-1* is expressed in the tail-spike cell.
A ~4kb promoter fragment from intron 1 of the *dre-1* locus drives GFP expression in the tail-spike cell. Two representative L1 animals are shown expressing *ced-3p*::NLS-RFP to mark the tail-spike cell, *dre-1p*::NLS-GFP to mark *dre-1*-expressing cells and the merged image to show their overlap in the binucleate tail-spike cell. Arrows point of the tail-spike cell. Both animals contain the *ced-3(n717)* mutation to allow visualization of the tail-spike cell in larvae.

dre-1 interacts genetically with core cell death pathway genes

Our results to this point suggest that *dre-1* acts as a pro-apoptotic molecule in the tail-spike cell to regulate developmental cell death. If this is the case, we would expect that it would interact genetically with alleles of the core apoptotic machinery, and the result might be a synergistic increase in tail-spike cell survival. As an example, combining a weak *ced-3* allele *(n2436)* with the *ced-9(n1950)* gain-of-function allele leads to a significant rise in the number of animals with a surviving tail-spike cell; *ced-3(n2436)* animals have 59% inappropriate survival, *ced-9(n1950)* animals have 3% survival, and *ced-3(n2436);ced-9(n1950)* animals exhibit 93% tail-spike cell survival (Fig. 16). Thus, weakening two parts of the core apoptotic machinery – EGL-1's ability to inhibit CED-9 and the caspase's ability to dismantle the cell – leads to a synergistic increase in survival. We wondered whether a similar effect would occur using *dre-1* alleles.

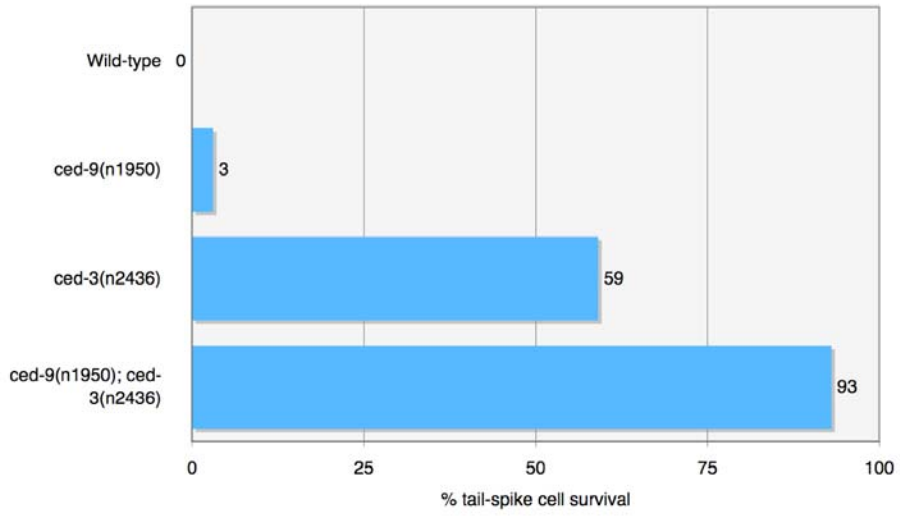

Fig. 16. Combining weak loss-of-function mutations in two apoptotic regulators leads to a synergistic increase in tail-spike cell survival. Reproduced from (Maurer et al., 2007).

Combining *ced-3* and *dre-1* alleles does in fact create a synergistic increase in the cell death defect. For example, while *ced-3(n2427);nsIs25* animals have 0% tail-spike cell survival, and *dre-1(dh99);nsIs25* animals 12%, *dre-1(dh99);ced-3(n2427);nsIs25* animals have 46% tail-spike cell survival (Fig. 17). Thus, *dre-1(lf)* mutants are a sensitized background with respect to tail-spike cell death, and in the presence of a weakened caspase, the cell survives at a greatly increased rate.

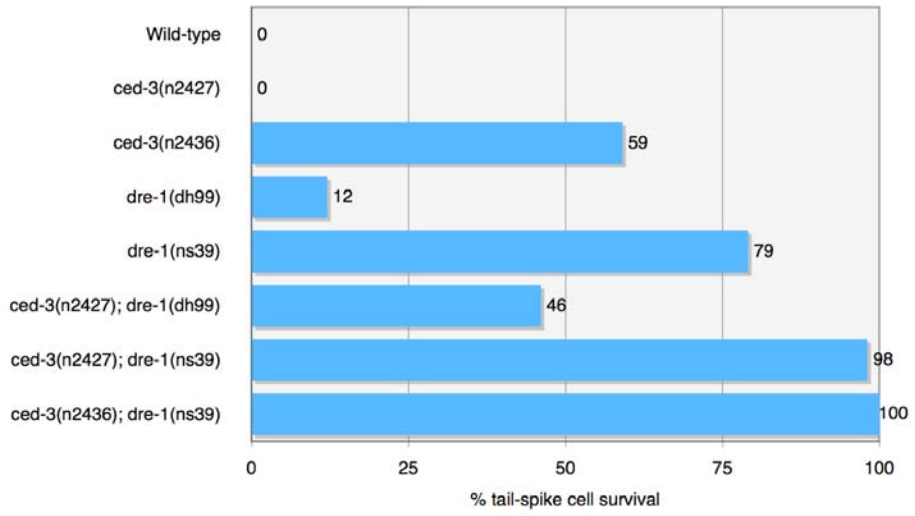

Fig. 17. *dre-1; ced-3(weak)* double mutants display a synergistic increase in tail-spike cell survival.
Percent of animals with a surviving tail-spike cell in strains with the indicated genotypes (n>100 for each). All strains contain the *nsIs25* transgene to mark the tail-spike cell.

Only one weak *ced-4* allele exists, *n3158*, and a similar analysis showed a similar synergistic effect (Fig. 18).

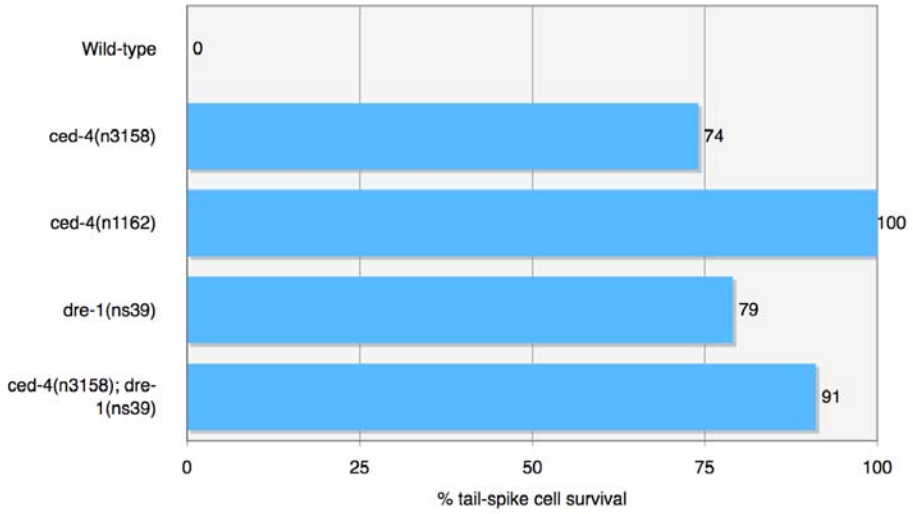

Fig. 18. *dre-1; ced-4(weak)* double mutants display a synergistic increase in tail-spike cell survival.
Percent of animals with a surviving tail-spike cell in strains with the indicated genotypes (n>100 for each). All strains contain the *nsIs25* transgene to mark the tail-spike cell.

The *ced-9(n1950)* gain-of-function allele disrupts EGL-1 binding to CED-9, creating a constitutive inhibitor of cell death. While this allele has, on its own, a relatively weak effect on tail-spike cell death, it displays a synergistic increase in tail-spike cell survival in the absence of full *dre-1* activity (Fig. 19).

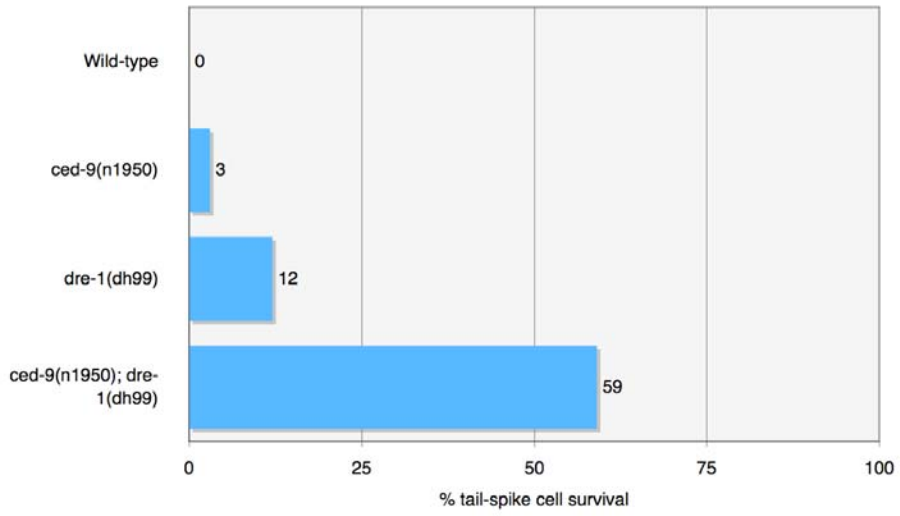

Fig. 19. *dre-1; ced-9(n1950)* double mutants display a synergistic increase in tail-spike cell survival.
Percent of animals with a surviving tail-spike cell in strains with the indicated genotypes (n>100 for each). All strains contain the *nsIs25* transgene to mark the tail-spike cell.

Carine Maurer showed that *egl-1* is dispensable for tail-spike cell death: in *egl-1*(null) mutants, the tail-spike cell dies in 70% of animals. This result raises the question of what is substituting for *egl-1* in the tail-spike cell to regulate caspase activation? Could *dre-1* be responsible for this activity? If so, we would again expect a synergistic effect of combining an *egl-1* mutation with *dre-1* mutations. This is in fact what we see, as double mutant combinations show increased tail-spike cell survival (Fig. 20).

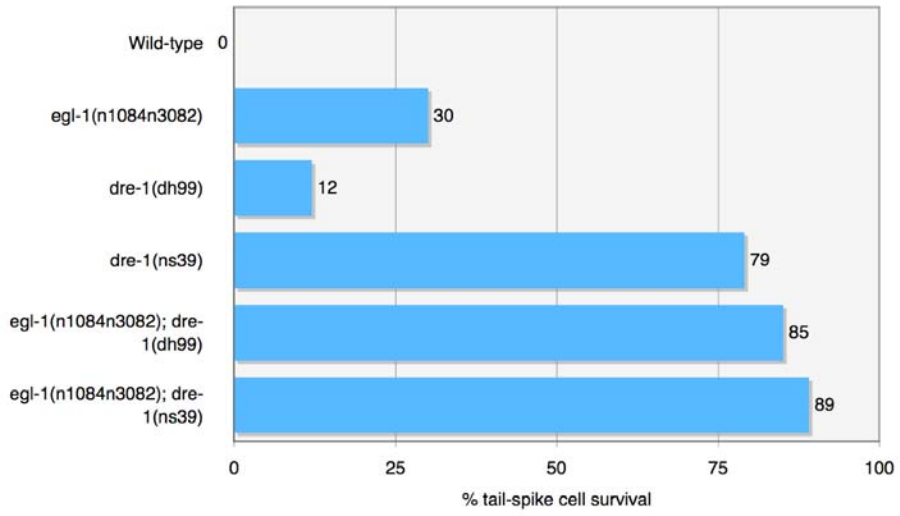

Fig. 20. *dre-1; egl-1(null)* double mutants display a synergistic increase in tail-spike cell survival.
Percent of animals with a surviving tail-spike cell in strains with the indicated genotypes (n>100 for each). All strains contain the *nsIs25* transgene to mark the tail-spike cell.

These results showing that *dre-1* mutations enhance mutations in pro-apoptotic genes are consistent with *dre-1* acting as a bona fide apoptotic regulator in the tail-spike cell. We wondered whether *ced-9*, the major anti-apoptotic molecule in *C. elegans*, would also interact genetically with *dre-1*. Constructing strains with the *ced-9(n2812)* allele is complicated by the fact that *ced-9(n2812)* homozygotes are inviable due to excess cell death; thus, a weak *ced-3* allele must always be present in the background to bypass this defect. Comparing *dre-1(ns39);ced-3(n2427)* animals to *ced-9(n2812);dre-1(ns39);ced-3(n2427)* animals shows a marked decrease in cell survival, with the levels closer to *ced-3(n2427)* alone (Fig. 21). This experiment demonstrates an epistatic relationship between *ced-9* and *dre-1* with respect to tail-spike cell death: in the absence of *ced-9*, *dre-1* status is largely irrelevant.

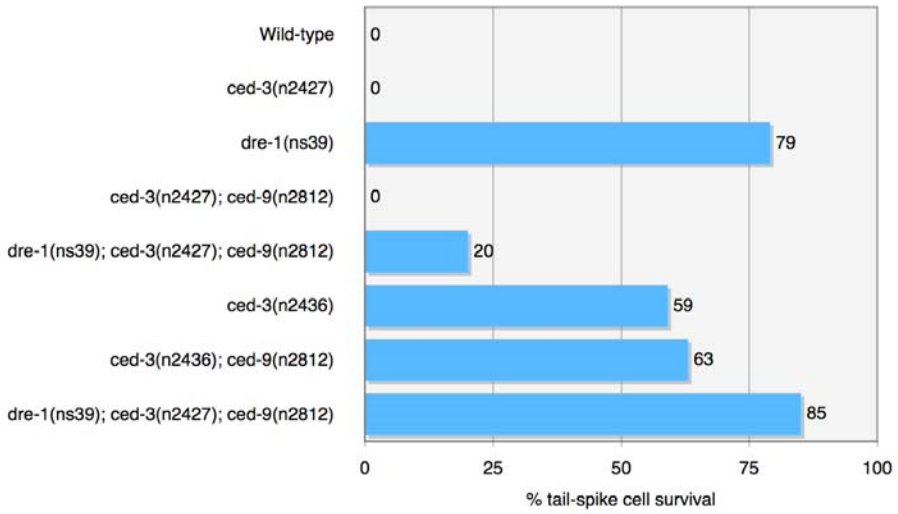

Fig. 21. *dre-1* acts upstream of, or in parallel to, *ced-9.*
Percent of animals with a surviving tail-spike cell in strains with the indicated genotypes (n>100 for each). All strains contain the *nsIs25* transgene to mark the tail-spike cell.

This result tells us several things. First, it shows that *ced-9*, despite *egl-1*'s minor role in tail-spike cell death, retains its anti-death function in this cell. Before we uncovered *dre-1*'s function in tail-spike cell death, the only role for *ced-9* was evident in *egl-1(n1084n3082);ced-9(n2812);ced-3(n2427)* animals, where the cell dies 100% of the time and which shows that *egl-1* acts through *ced-9* to promote death, albeit in a minor role. Second, this result shows that *dre-1* acts upstream of, or in parallel to, *ced-9* to control tail-spike cell death. Third, it shows that *dre-1* may have a role as a controller of cell death through a different pathway, as 20% of animals retain a surviving tail-spike cell in this strain. Thus, even in the absence of *ced-9*, *dre-1* still affects cell death.

The homeodomain transcription factor *pal-1* is required for tail-spike cell death as a transcriptional activator of *ced-3* just prior to death (Maurer et al., 2007), which, given that *dre-1* appears to act upstream of or in parallel to *ced-9*, would suggest that *pal-1* should be epistatic to *dre-1*. *pal-1;dre-1* double mutants support this prediction, as they show diminished *ced-3pro::gfp* expression (Fig. 22). These results are consistent with *dre-1* acting upstream of or in parallel to *ced-9* and *pal-1* activation of *ced-3* transcription being far downstream in the cascade of tail-spike cell death.

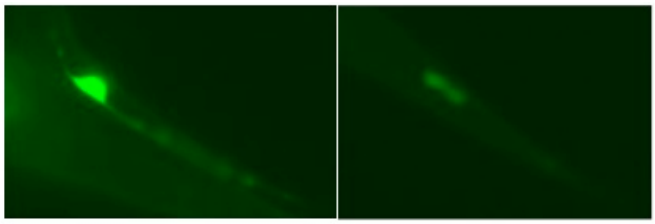

dre-1(dh99) *dre-1(dh99); pal-1(ns114)*

Fig 22. *pal-1* is epistatic to *dre-1* with respect to *ced-3* transcription. One second exposures of surviving tail-spike cells in *dre-1(dh99)* and *dre-1(dh99);pal-1(ns114)* animals. Note that GFP expression is significantly dimmer in the *pal-1* mutant, as would be expected if it is acting downstream to regulate *ced-3* transcription. Both animals contain the *nsIs25 ced-3pro::gfp* transgene to visualize *ced-3* transcription.

Because of *pal-1*'s effects on *ced-3* transcription, *pal-1* mutants also display a tail-spike cell death defect, with 30% of animals showing a surviving tail-spike cell in *pal-1(ns114)* animals. Scoring tail-spike cell survival in these animals is complicated by the fact that the *ns114* mutation reduces *ced-3pro::gfp* expression in the tail-spike cell, making it difficult to discern whether the tail-spike cell has survived. The reduced *ced-3pro::gfp* is incompletely penetrant, however, making it possible to see the tail-spike cell in some animals, with the caveat that this is an underestimate of tail-spike cell survival. Despite that limitation, we were able to see an increase in tail-spike cell survival when combining *pal-1* and *dre-1* mutants, consistent with both having partial effects on tail-spike cell death (Fig. 23).

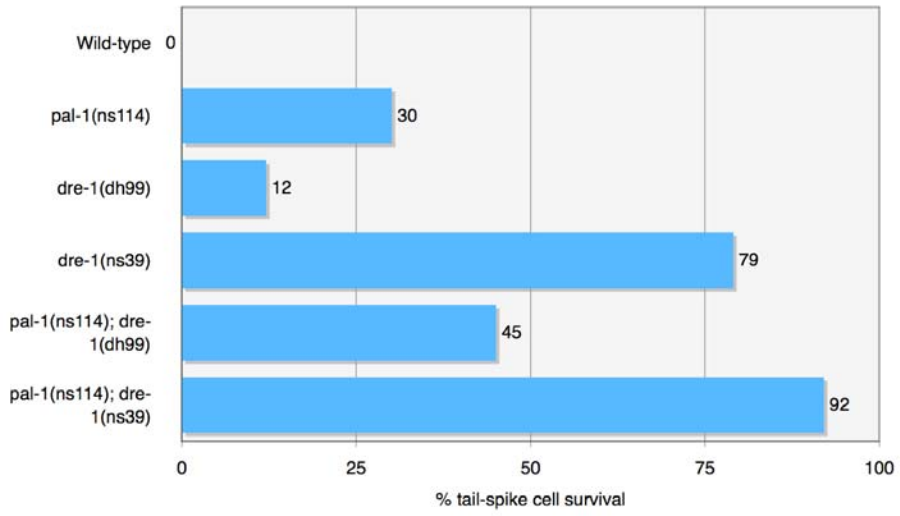

Fig. 23. *dre-1; pal-1(ns114)* double mutants display an increased tail-spike cell death defect.
Percent of animals with a surviving tail-spike cell in strains with the indicated genotypes (n>100 for each). These numbers are an underestimate because they do not count animals in which the *pal-1* mutation completely abolished *ced-3pro::gfp* transcription in the tail-spike cell, which we are unable to score. All strains contain the *nsIs25* transgene to mark the tail-spike cell.

dre-1 does not regulate pharyngeal cell death

Having established *dre-1* as a regulator of apoptosis in the tail-spike cell, we wondered whether it plays a similar role in other cells. To address this, we used the pharynx assay, in which the number of cells present in the anterior pharynx is counted under DIC microscopy. In animals with mutations in the core apoptotic machinery, as many as 14 extra cells accumulate in the anterior pharynx, and this assay allows quantification of the global cell death defect. These assays were performed by Shai Shaham.

First, we addressed whether *dre-1(ns39)* animals had extra cells in the pharynx (Table 1). As we expected from initial experiments by Carine Maurer described above in which mutants from the screen were secondarily screened by checking for a global cell death defect, *dre-1(ns39)* animals had no extra cells in the pharynx. This result is also unsurprising considering that *dre-1* was not isolated in any screens for global cell death defects based on the pharyngeal cell death assays.

We looked for other evidence that *dre-1* plays a role in pharyngeal cell death by asking whether the *dre-1(ns39)* mutation could enhance the death defect of weak *ced-3* alleles: *dre-1* might have a supporting role in promoting death which might only be uncovered in the setting of weakened caspase activity. However, *dre-1(ns39);ced-3(n2436)* animals did not show an increased number of cells in the pharynx suggesting that *dre-1* may not play a part in these cell deaths (Table 1). As a parallel experiment, we tested whether *egl-*

1(n1084n3082)/+; *dre-1(n39)*/+ animals had extra cells in the pharynx, as our tail-spike cell data suggest that *dre-1* acts upstream of *ced-9*, in place of *egl-1*. Again, no extra cells were found in the pharynxes of these animals, making it unlikely that *dre-1* is a major player in pharyngeal cell death (Table 1). Thus, we conclude that *dre-1* is required for tail-spike cell, but not pharyngeal cell death.

Genotype	# extra cells
ced-3(n2436)	4.2
dre-1(ns39)	0
ced-3(n2436); dre-1(ns39)	3.7
dre-1(ns39)/+; *egl-1(n1084n3082)*/+	0

Table 1. The *dre-1(ns39)* mutation does not affect cell death in the pharynx.
Global cell death was assessed in the anterior pharynx in *ced-3(n2436)*, *dre-1(ns39)*, *ced-3(n2436);dre-1(ns39)* double mutants and *dre-1(ns39)*/+;*egl-1(n1084n3082)*/+ heterozygotes. No effect was seen in *dre-1* mutants (counts performed by Shai Shaham).

C05C8.6, a BTB/POZ domain protein, may play a minor role in tail-spike cell death

A high-throughput yeast two-hybrid screen of thousands of *C. elegans* proteins showed that DRE-1 interacts with C05C8.6 in this assay (Li et al., 2004). C05C8.6, a BTB/POZ domain protein, remains uncharacterized, but the fact that it contains a BTB domain was intriguing to us, considering the role that BTB domain-containing proteins have in the ubiquitin-proteasome system. In addition, Li et al. reported that C05C8.6 interacts with itself; GLY-4, a predicted UDP-galNAc-ase; GST-24, a glutathione transferase; RAD-26, a helicase; and F52B11.1, a PHD Zn-finger protein. Alleles are available for *C05C8.6*, *gly-4* and *gst-24*, and we tested whether any of these had an effect on tail-spike cell death.

On their own, mutations in none of *C05C8.6*, *gly-4* or *gst-24* blocked tail-spike cell death, with 1%, 1% and 1.5% of animals having an inappropriately surviving tail-spike cell, respectively (Fig. 24). We tested whether these mutations had any effect on tail-spike cell death in the context of the *dre-1(ns39)* mutation. *C05C8.6(tm3719)* had a slight suppressive effect on tail-spike cell death in the *C05C8.6(tm3719); dre-1(ns39)* double mutant: 59% vs. 79% inappropriate survival (Fig. 24). This suppression could suggest that *C05C8.6* acts downstream of, or in parallel to *dre-1* to regulate tail-spike cell death, but such a weak effect is difficult to interpret, and could also be due to other mutations in the background. *gly-4(ok2943)* enhanced tail-spike cell survival slightly when combined with the *dre-1(ns39)* mutation, increasing survival from

79% to 87% (Fig. 24). Again, this weak enhancement of tail-spike cell survival is difficult to interpret, although the fact that *dre-1* contains three CASH domains reported to be involved in carbohydrate binding makes *gly-4* an intriguing gene. *gst-24(ok3042)* had no significant effect on the *dre-1(ns39)* mutant, with tail-spike cell survival of 70% vs. 79%. We conclude that *C05C8.6* may play a minor role in tail-spike cell death, and *gly-4* may as well, while *gst-24* is unlikely to be involved in this process.

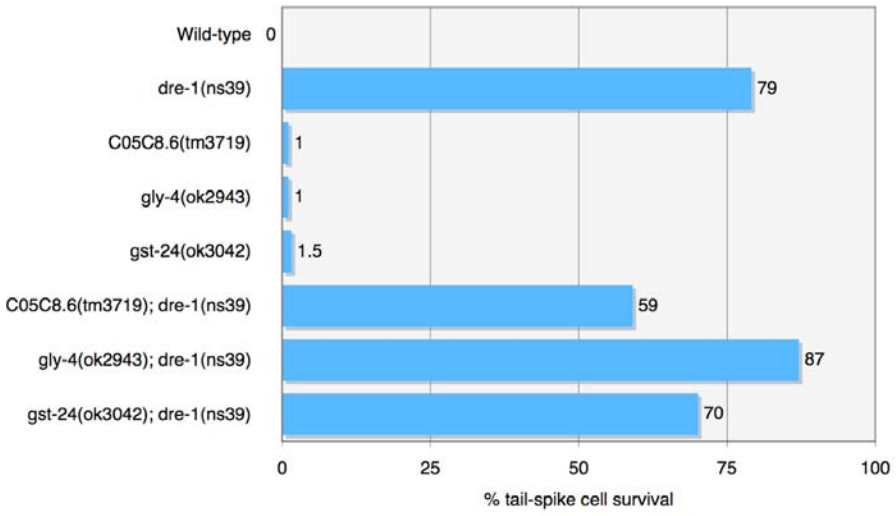

Fig. 24. *C05C8.6* and its putative interacting partners play a minor or negligible role in tail-spike cell death.
Percent of animals with a surviving tail-spike cell in strains with the indicated genotypes (n>100 for each). All strains contain the *nsIs25* transgene to mark the tail-spike cell.

Tail-spike cell death is not affected by heterochronic genes but may be subtly controlled by a microRNA

The *dre-1* 3'UTR contains several putative microRNA binding sites as predicted by various online tools. *mir-2* and *mir-71* have high scores for complementarity and alleles exist for both of these genes. To test whether *mir-2* or *-71* have a role in tail-spike cell death, we crossed both of these mutants to the tail-spike cell GFP reporter, *nsIs25*. Neither *mir-2;nsIs25* nor *mir-71;nsIs25* animals had any evidence of tail-spike cell survival (Fig. 25). We also tested whether *mir-71* interacted genetically with *dre-1* in any way. Surprisingly, *mir-71;dre-1(ns39);nsIs25* animals had an enhanced tail-spike cell death defect, suggesting that *mir-71* may have a weak pro-death effect that is only unmasked in the context of the *dre-1* mutant.

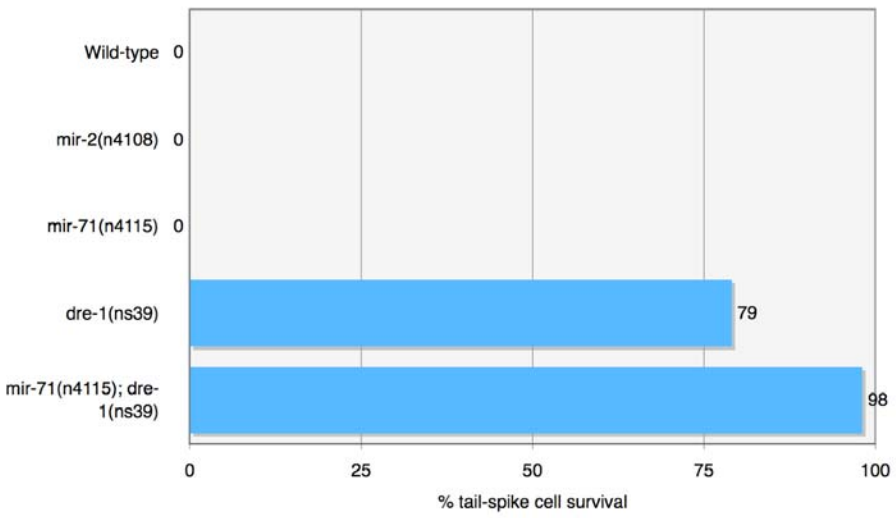

Fig. 25. A *mir-71* mutation enhances the tail-spike cell death defect in *dre-1(ns39)* animals.
Percent of animals with a surviving tail-spike cell in strains with the indicated genotypes (n>100 for each). All strains contain the *nsIs25* transgene to mark the tail-spike cell.

dre-1 was isolated from a screen for enhancers of a *daf-12* mutation's effect on heterochronic phenotypes (distal tip cell migration and seam cell fusion). The genes *lin-4*, *lin-46*, *lin-29* and *lin-28* have been implicated in these processes and thus we wondered whether there was a connection between tail-spike cell death and any of these genes. Crossing each to the *nsIs25* tail-spike cell marker showed that none of the resulting strains had tail-spike cell death defects (Fig. 26). With this result, in concert with the fact that all heterochronic phenotypes are post-embryonic while tail-spike cell death occurs during embryogenesis, we conclude that *dre-1*'s role in regulating tail-spike cell death is independent of these heterochronic pathways.

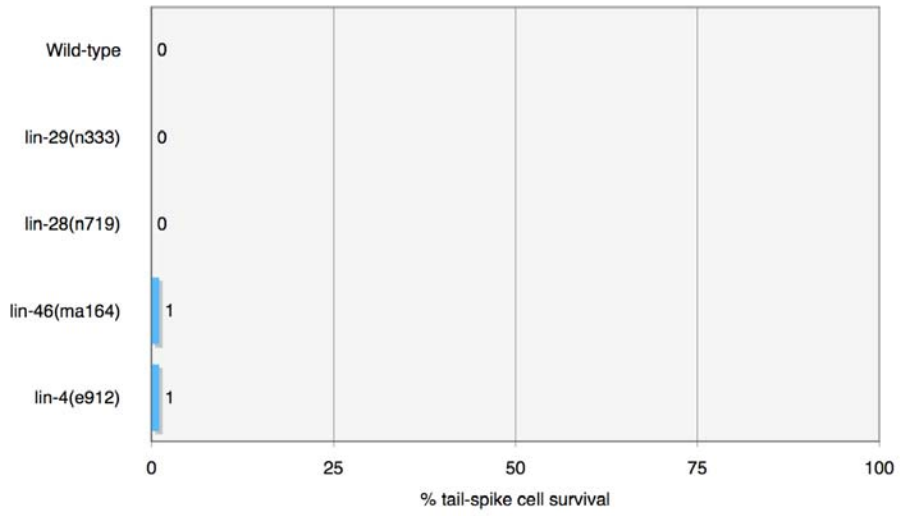

Fig. 26. *dre-1* does not act in a heterochronic pathway to regulate tail-spike cell death.
Percent of animals with a surviving tail-spike cell in strains with the indicated genotypes (n>100 for each). All strains contain the *nsIs25* transgene to mark the tail-spike cell.

3.3 Conclusions

The major draw of studying the tail-spike cell is that, while its death requires *ced-3* caspase activation through ced-4, *egl-1* plays a relatively minor role in controlling *ced-3* activation. Thus, the power of *C. elegans* genetics can be used to identify novel genes that influence caspase activation, and act in *egl-1*'s stead.

Several lines of evidence show that *dre-1* is a bona fide cell death regulator in the tail-spike cell, and is in fact a substitute for *egl-1*. First, mutations in *dre-1* block tail-spike cell death and these mutations can be rescued by cell autonomous expression of wild-type *dre-1*. We would expect that, like the core cell death machinery, *dre-1* would act in the cell that it was involved in killing. Second, the *dre-1(ns39)* mutation blocks tail-spike cell death in most animals, but in those animals in which the cell dies, the death appears normal, and a classically apoptotic corpse is evident by DIC microscopy. Also, in those animals in which the tail-spike cell survives, it is morphologically indistinguishable from a surviving tail-spike cell seen in a *ced-3*, *ced-4* or *egl-1* mutant. Thus, *dre-1(ns39)* does not cause a cell fate change such that the embryonic lineage is altered and the cell is never born or becomes a drastically altered cell. Third, mutations in *dre-1* synergize with mutations in core cell death components, suggesting that the *dre-1* mutant background is sensitized with respect to tail-spike cell death. Furthermore, the genetic results show that *dre-1* acts upstream of, or in parallel to *ced-9* to regulate tail-spike cell death, and that *pal-1* is downstream of *dre-1* as

well. These results do not address how *dre-1* controls tail-spike cell death, but the domain structure of *dre-1* hints at a role as an E3 ligase for the ubiquitin-proteasome system.

Chapter 4: DRE-1 acts in an SCF complex to regulate tail-spike cell death

4.1 Background

The ubiquitin-proteasome system is the major control over protein turnover in eukaryotic cells, and as such plays a crucial role in all biologic processes. The ability to precisely affect levels of individual proteins within the cellular environment allows fine tuning of cellular functions. Among the most important processes to precisely control is cell death, as cell death regulators represent the seeds of a cell's demise lurking within at all times. Caspase activation in the wrong time and place can have disastrous implications for the organism, considering the feed forward mechanism built into the system. In light of this, many levels of regulation have been built into the caspase activation process, including many examples of ubiquitin-proteasome related control. The most important cell death-related ubiquitin ligases are the IAPs, which, in vertebrates and *Drosophila*, are vital regulators of caspases. IAPs are RING domain-

containing E3s, however, a different class of molecule from *dre-1*, which is an F box protein. F box proteins are known to act as E3s through a multi-subunit complex, the SCF complex. In these complexes, the E2-recruiting RING domain is supplied by an Rbx1/Roc1-like protein, which binds to a cullin scaffolding protein. The cullin, in turn, binds to a SKP1-like protein which binds to the F box protein via the F box domain. The F box protein supplies the specificity of the SCF E3 ligase, binding via its C-terminus to the substrate and bringing the target into position for ubiquitin to be conjugated to lysine residues in the polypeptide. To date, no SCF complexes have been reported as regulators of programmed cell death in *C. elegans*.

4.2 Results

Knockdown of *dre-1*, *skr-1* or *cul-1* prevent tail-spike cell death

dre-1 contains an F box near the N-terminus, known to bind to Skp1-like proteins which, along with cullin-like and rbx1-like proteins form an SCF complex to ubiquitinate target proteins. Several lines of evidence suggested to us that *dre-1* may act in an SCF complex regulate tail-spike cell death. First, in all organisms harboring a *dre-1*-like gene, the F box is highly conserved. For example, comparing *C. elegans dre-1* to human FBXO11 with the ClustalW tool, 16/41 residues are identical (39%), 12/41 residues are conserved based on charge and size (29%) and 7/41 are semi-conserved based on steric size and

shape (17%), bringing the total identical + conserved + semi-conserved to 35/41 (85%). Second, the strongest allele affecting tail-spike cell death (*ns39*) is a substitution in the F box changing a semi-conserved serine to a leucine (a residue of a different chemical class). This serine is adjacent to a valine which is conserved in all organisms examined except *Nematostella vectensis* (sea anemone). This valine is conserved in human, mouse, rat, *Drosophila melanogaster*, *Xenopus laevis*, *Caenorhabditis brenneri*, *Caenorhabditis briggsae*, *Caenorhabditis japonica*, *Caenorhabditis remanei*, *Brugia malayi*, zebrafish, *Tetraodon nigroviridis* (pufferfish), *Aedes aegypti*, *Anopheles gambiae*, *Ixodes scapularis* (black-legged tick), and *Ciona intestinalis* (sea squirt). Third, Fielenbach et al. reported that dre-1 physically interacts with SKR-1 and SKR-2 but not SKR-3, -4, -5, -7, -8, -9, -10, -12, -13, -14, -15, -17, -19, -20 or -21 in a yeast two-hybrid assay and that RNAi against *skr-1*, *cul-1* and *rbx-1/2* recapitulated the *dre-1* heterochronic phenotype.

While this is suggestive of *dre-1* acting in an SCF complex to regulate tail-spike cell death, we wanted to test the hypothesis directly by assessing the role of individual SCF genes in a reverse genetic manner. To do so, we had to develop a method for screening a defined set of genes for a role in tail-spike cell death. Using the RNAi feeding library available in the laboratory, we found that L4s and gravid young adults carrying an RNAi-sensitizing *rrf-3(pk1426)* mutation placed on a lawn of RNAi-expressing *E. coli* gave the strongest tail-spike cell death phenotype. Feeding animals *ced-4* RNAi in this assay resulted in 20% tail-

spike cell survival illustrating that the penetrance of RNAi effects in this cell are incomplete (compare to the 100% survival in *ced-4(n1162 animals)*), but significant compared to empty-vector bacteria (0% survival) (Fig. 27). In addition to *ced-4*, a second positive control for this assay was *dre-1*, which gave 10% survival.

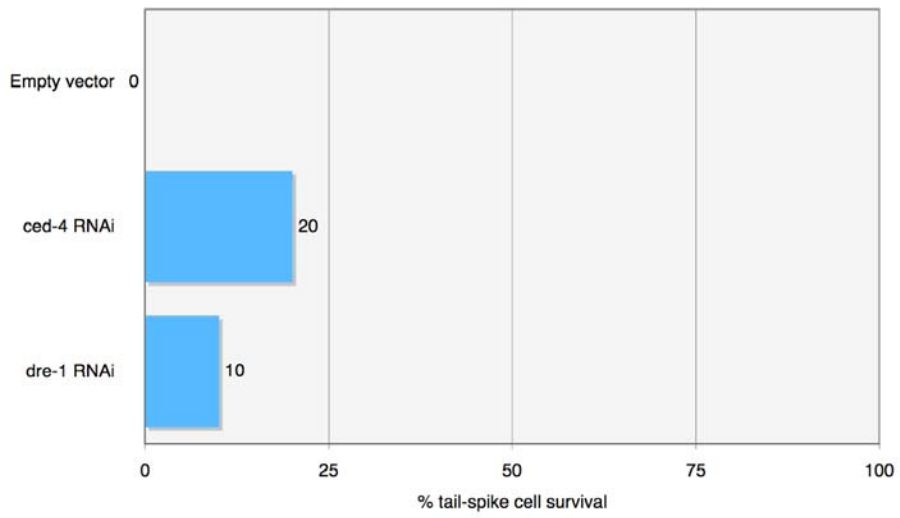

Fig. 27. Knockdown of *ced-4* and *dre-1* by feeding RNAi induces a partial tail-spike cell defect.
L4 and gravid adults of the *rrf-3(pk1426); nsIs25* genotype were placed on lawns of bacteria expressing empty vector, *ced-4* RNAi and *dre-1* RNAi. L1 progeny were scored for tail-spike cell survival one and two days later (n>100 for each).

With this method established, we tested the effect of knocking down *skr-1, -2, -3, -5, -7, -8, -9, -11, -12, -13, -15, -17, -18, -19, -20, rbx-1, rbx-2, cul-1, -4, -5,* and *-6*. Of these genes, only *cul-1* gave a significant phenotype: 9% tail-spike cell survival (Fig. 28). This result is on par with the level of survival of animals grown on *dre-1* RNAi, in which the tail-spike cell survives in 10% of animals. None of the *skr* genes gave a significant cell death phenotype, with *skr-1* giving the largest effect, 2%.

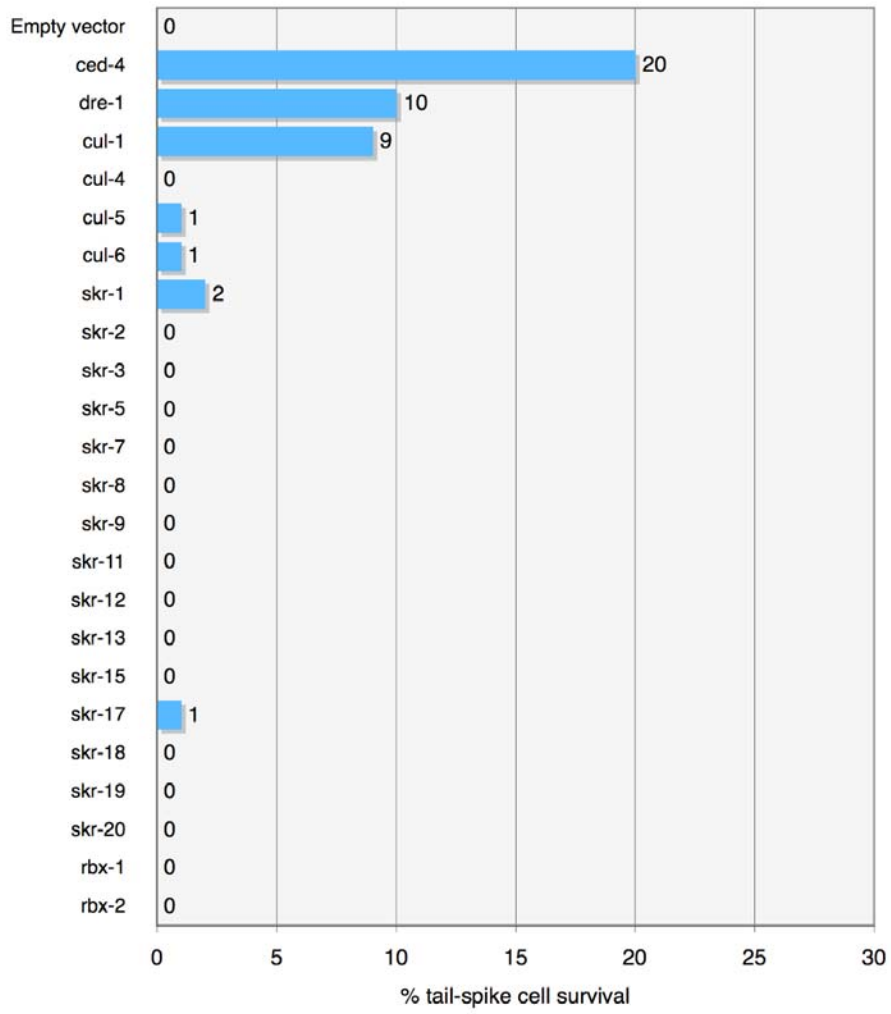

Fig. 28. Knockdown of *cul-1* by feeding RNAi induces a partial tail-spike cell defect.
L4 and gravid adults of the *rrf-3(pk1426); nsIs25* genotype were placed on lawns of bacteria expressing the indicated RNAi. L1 progeny were scored for tail-spike cell survival one and two days later (n>100 for each).

Given that *skr-1* and *-2* were reported by Fielenbach et al. to interact with *dre-1* in a yeast two-hybrid assay, and *skr-1* RNAi had a very weak effect on tail-spike cell death, we tested two genetic alleles of *skr-1* for tail-spike cell phenotypes. A deletion allele, *ok1696*, of *skr-1* is viable as a homozygote with occasional dpy animals present on the plate. *skr-1(ok1696);nsIs25* animals had 0% tail-spike cell survival, suggesting that either (1) *skr-1* plays no role in tail-spike cell death, (2) *skr-2* or another gene is redundant and takes over in its absence, or (3) this allele is not a true null for *skr-1*. Several lines of evidence suggest that the correct explanation is the third. First, injection of *skr-1* RNAi into hermaphrodite gonads produces embryonic lethality of most progeny due to hyperplasia during development (Yamanaka A et al., 2002; Nayak S et al., 2002), suggesting that the true phenotype of *skr-1(null)* is embryonic lethality and that the fully viable *ok1696* allele is not a null. Second, another deletion allele which we have not yet obtained, *tm2391*, is reported to be inviable as a homozygote and fails to complement the *skr-1(sm151)* point mutant (Killian DJ et al., 2008). Third, the *skr-1(sm151)* mutation, a weak semidominant allele that is viable, gives 4% tail-spike cell survival, compared to 0% for *nsIs25* alone (Fig. 29). This result shows that *skr-1* (and possibly its close relative *skr-2*) is required for tail-spike cell death.

A *cul-1* allele (*e1756*) exists that has a sterile phenotype as a homozygote: *cul-1* is maternally provided from a heterozygous mother to her homozygous progeny, who display a lon phenotype and whose progeny are embryonic lethal

due to lack of *cul-1*. Because of this lethality phenotype, we were only able to score sterile animals, and of these, 0% had a surviving tail-spike cell (Fig. 29). With these limitations, we are unable to test genetically *cul-1*'s role in tail-spike cell death, but given the RNAi phenotype, and that Fielenbach et al. also described a *cul-1* RNAi phenotype for *dre-1*-related processes, we conclude that *dre-1* acts in an SCF complex made up of *dre-1*, *skr-1*, *cul-1* (and presumably *rbx-1* and/or *-2*) to regulate tail-spike cell death.

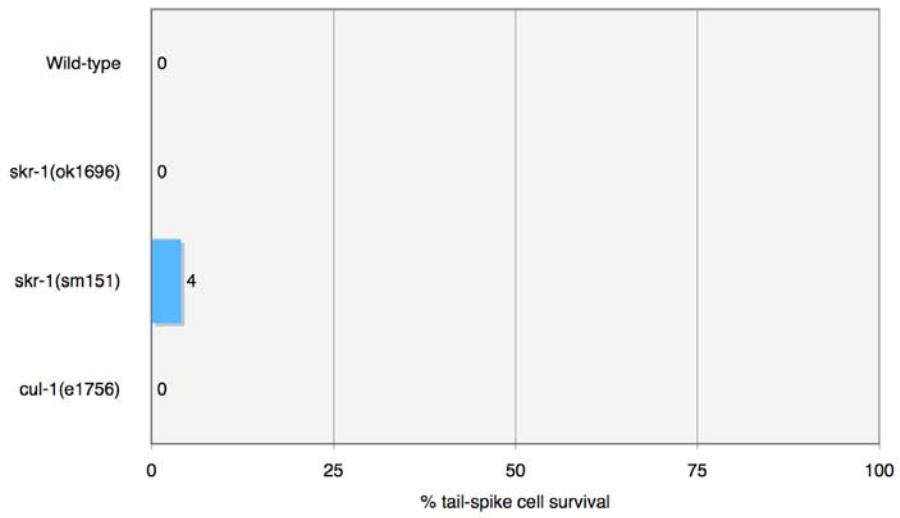

Fig. 29. The *skr-1(sm151)* weak loss-of-function allele weakly blocks tail-spike cell death.
Percent of animals with a surviving tail-spike cell in strains with the indicated genotypes (n>100 for each). All strains contain the *nsIs25* transgene to mark the tail-spike cell.

Abida et al. reported that *dre-1*'s human homolog, FBXO11, has the capability to neddylate proteins (Abida et al., 2007). We tested whether RNAi against the *C. elegans* nedd (*ned-8*) affected tail-spike cell death. 0% of animals grown on *ned-8* RNAi had surviving tail-spike cells, and we conclude that *ned-8* is not required for tail-spike cell death (Fig. 28).

DRE-1 physically interacts with SKR-1 via the F box

These genetic data suggest a model in which DRE-1 binds to SKR-1 (and possibly SKR-2) which binds to CUL-1 and the remainder of the SCF complex to regulate tail-spike cell death. As in other DRE-1-like proteins and their interactions with SKP-like proteins, the DRE-1-SKR-1 interaction should require an intact F box domain but not CASH domains. To test this hypothesis, I performed immunoprecipitation experiments with myc- and HA-tagged forms of these proteins expressed in *Drosophila* Schneider S2 cells (Fig. 29). Immunoprecipitation with anti-HA-agarose beads successfully enriched for HA-tagged DRE-1, DRE-1(ns39), DRE-1(dh99). Western blot analysis for myc-tagged SKR-1 showed that HA::DRE-1 and HA::DRE-1(dh99) but not HA::DRE-1(ns39) or myc::SKR-1 alone immunoprecipitated myc::SKR-1. That both the HA::DRE-1 and HA::DRE-1(dh99) proteins bound myc::SKR-1 but not HA::DRE-1(ns39) are consistent with the F box being required for DRE-1-SKR-1 binding and gives biochemical logic to the genetic phenotypes of the *dre-1(ns39)* and *dre-1(dh99)* mutants.

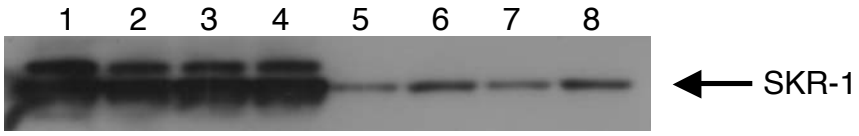

anti-myc immunoblot

Lane 1: myc::SKR-1 + 0, input
Lane 2: myc::SKR-1 + HA::DRE-1, input
Lane 3: myc::SKR-1 + HA::DRE-1(ns39), input
Lane 4: myc::SKR-1 + HA::DRE-1(dh99), input
Lane 5: myc::SKR-1 + 0, IP anti-HA
Lane 6: myc::SKR-1 + HA::DRE-1, IP anti-HA
Lane 7: myc::SKR-1 + HA::DRE-1(ns39), IP anti-HA
Lane 8: myc::SKR-1 + HA::DRE-1(dh99), IP anti-HA

Fig. 30. DRE-1 binds to SKR-1 and the *ns39* F box mutation inhibits this interaction.
myc::SKR-1 was expressed alone or in the presence of wild-type HA::DRE-1, HA::DRE-1 with the F box mutation (*ns39*), or HA::DRE-1 with the CASH domain mutation (*dh99*). Immunoprecipitation was performed using anti-HA beads to enrich for HA::DRE-1 proteins, and immunoblotting was performed with anti-myc antibodies to detect myc::SKR-1. The F box mutation affects SKR-1 binding to DRE-1, but the C-terminal CASH domain mutation does not.

NB: I plan to replace this blot with one that is better exposed in the coming weeks.

4.3 Conclusions

Our results show that DRE-1, in concert with SKR-1, CUL-1, and, most likely, RBX-1/2 form an SCF complex to regulate tail-spike cell death. Via either RNAi knockdown or genetic alleles we were able to observe tail-spike cell effects of loss of *dre-1*, *skr-1* and *cul-1*. In addition, our biochemical studies suggest that the interaction of DRE-1 with SKR-1 is mediated by the F box, and that the *dre-1(ns39)* missense mutation affects this binding, while the *dre-1(dh99)* mutation does not. These results are in line with earlier expression experiments which suggested that *skr-1* and *cul-1* are ubiquitous proteins, expressed during embryogenesis. While these data show that the *dre-1* SCF complex is an important regulator of tail-spike cell death, and establish this E3 ligase as the first to our knowledge to be involved with programmed cell death in *C. elegans*.

Chapter 5: DRE-1/FBXO11 is mutated or deleted in human lymphomas and may interact with CED-9/BCL2 to induce its degradation

5.1 Background

Evasion of apoptosis is a requirement of every cancer cell, as the accumulation of genotoxic stress, hypoxia, lack of growth factors and other insults should lead to the apoptotic removal of nascent tumor cells (Hanahan and Weinberg, 2000). However, as evidenced by the high rate of p53 mutations in almost all cancers (greater than 50%), as well as the incidence of BCL2 amplifications and translocations, these pro-death signals can be evaded through mutation. Indeed, BCL2 was first described as a translocation partner with the immunoglobulin heavy chain locus in the t(14;18) translocation found in follicular lymphoma. Further studies showed that BCL2 is dysregulated in many B cell lymphoma subtypes, including diffuse large B cell lymphoma, by translocation, genomic amplification and transcriptional upregulation (Lenz and Staudt, 2010).

Pro-apoptotic genes, such as p53, on the other hand, are frequently deleted or mutated to produce loss-of-function phenotypes, preventing apoptosis from proceeding. Because of the conserved nature of *dre-1* across metazoans, the central importance of *ced-9* as the only known anti-apoptotic gene in *C. elegans*, the epistasis results suggesting that *dre-1* acts upstream of or in parallel to *ced-9*, and the frequency of BCL2 dysregulation in human lymphoma, we investigated whether FBXO11 acts as a tumor suppressor in human lymphoma and whether DRE-1/FBXO11 regulates CED-9/BCL2 turnover.

5.2 Results

DRE-1 and CED-9 interact with low affinity in *Drosophila* S2 cells

To test whether DRE-1 and CED-9 interact physically, we expressed HA::DRE-1 in the presence or absence of myc::CED-9 in *Drosophila* S2 cells and used magnetic beads to immunoprecipitate myc::CED-9 and anti-HA immunoblotting to detect HA::DRE-1 in the lysates (Fig. 31). We observed a consistent increase in HA::DRE-1 detected in the lysates when myc::CED-9 was present compared with when myc::CED-9 was absent. However, HA::DRE-1 was also consistently weakly immunoprecipitated with anti-myc beads in the absence of myc::CED-9, and this non-specific interaction could not be eliminated by altering the wash buffer conditions as more stringent washes eliminated the specific interaction as well. Therefore, we are able to detect an interaction, albeit a weak one, between DRE-1 and CED-9 *in vitro*.

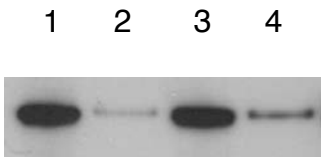

Anti-HA immunoblot.
Lane 1: HA::DRE-1 + 0, input
Lane 2: HA::DRE-1 + 0, IP anti-myc
Lane 3: HA::DRE-1 + myc::CED-9, input
Lane 4: HA::DRE-1 + myc::CED-9, IP anti-myc

Fig. 31. DRE-1 and CED-9 interact with low affinity in *Drosophila* S2 cells. HA::DRE-1 was expressed alone (lanes 1 and 2) or together with myc::CED-9 (lanes 3 and 4). Immunoprecipitations were performed with anti-myc antibodies and immunoblotting with anti-HA antibodies to detect HA::DRE-1. While some non-specific binding is present in lane 2, a specific interaction is apparent in lane 4.

We also attempted to visualize CED-9 protein in the tail-spike cell, as one prediction from our model is that, in *dre-1(ns39)* mutants, CED-9 should accumulate due to a lack of *dre-1* SCF activity. We obtained an anti-CED-9 antibody from Barbara Conradt, and used two fixation and staining protocols to immunostain *ced-3(n2436)* and *dre-1(ns39);ced-3(n2436)* animals. We chose these strains as the *ced-3* mutation would allow visualization of the tail-spike cell

in L1 animals in *dre-1(wild-type)* animals; otherwise, the cell would have died in embryogenesis. Despite successful staining with another, unrelated antibody in these experiments (anti-AJM-1), we were unable to observe CED-9 staining in either strain. This could be due to faulty staining with the anti-CED-9 antibody, to CED-9 levels being at a level below detection even in *dre-1(ns39)* animals, or to the *dre-1(ns39)* mutation not having an effect on CED-9 protein levels.

FBXO11 is mutated or deleted in human lymphoma and these mutations cause reduced function

dre-1 is one of the few F box proteins which is conserved across metazoans, with 82% similarity to human FBXO11. Given this remarkable similarity, we wondered whether it plays a role in apoptosis in other organisms, and specifically whether it could function as a tumor suppressor in human cancer. In a serendipitous connection, I suggested this possibility to Dr. Louis Staudt at NCI, who noticed that certain lymphoma cell lines have deletions or mutations that affect the FBXO11 locus. The Farage cell line contains a double deletion that removes FBXO11, the MedB1 line has a single deletion, and OCI-Ly1 contains a missense mutation as well as a nonsense mutation. His group also identified mutations in FBXO11 when sequencing DNA derived from primary diffuse large B-cell lymphoma (DLBCL) tumor samples. Four mutations were found in germinal center-like DLBCL (GCB-DLBCL), representing 5% of tumors sequenced and two mutations were found in activated B-cell-like DLBCL (ABC-

DLBCL). These mutations, with the mouse ENU-derived mutation (Jeff) and the *C. elegans* mutations, are a mixture of missense mutations and nonsense mutations, and are summarized below (Fig. 32).

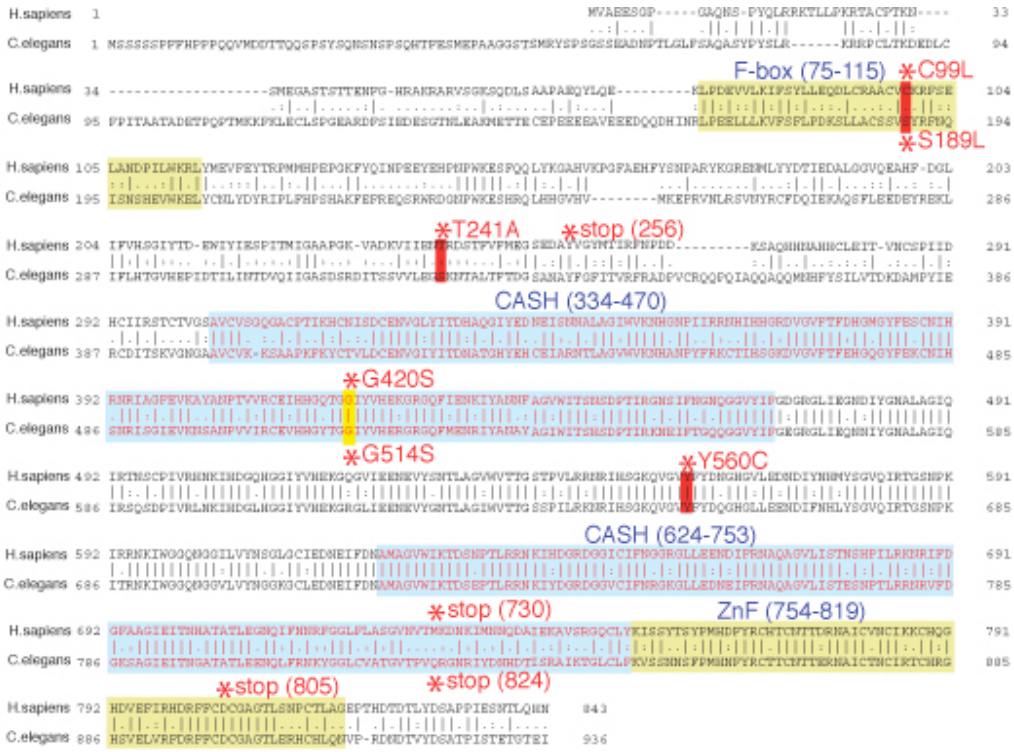

Fig. 32. *dre-1* and FBXO11 mutations from *C. elegans* mutants and patient samples.

We wondered whether these mutations would affect *dre-1* function in the tail-spike cell. To address this question, we expressed mutant forms of the *dre-1* cDNA in the tail-spike cell using the *aff-1* promoter and assessed their ability to rescue the *dre-1(ns39)* phenotype. The Y560C mutation found in a lymphoma cell line susceptible to FBXO11 expression (see below), corresponds to the Y2218C mutation in *C. elegans*. When modeled in the tail-spike cell, this mutant retained some rescue ability, but was less efficient at killing the tail-spike cell than the wild-type cDNA, resulting in 39, 41 and 45% tail-spike cell survival in three independent lines (Fig. 33). The human nonsense mutation at position 256 was even less effective at rescuing tail-spike cell death, with the cell surviving 65% of the time. These results show that the human mutations produce a hypomorphic protein, which is consistent with other loss-of-function mutations in tumor suppressor genes.

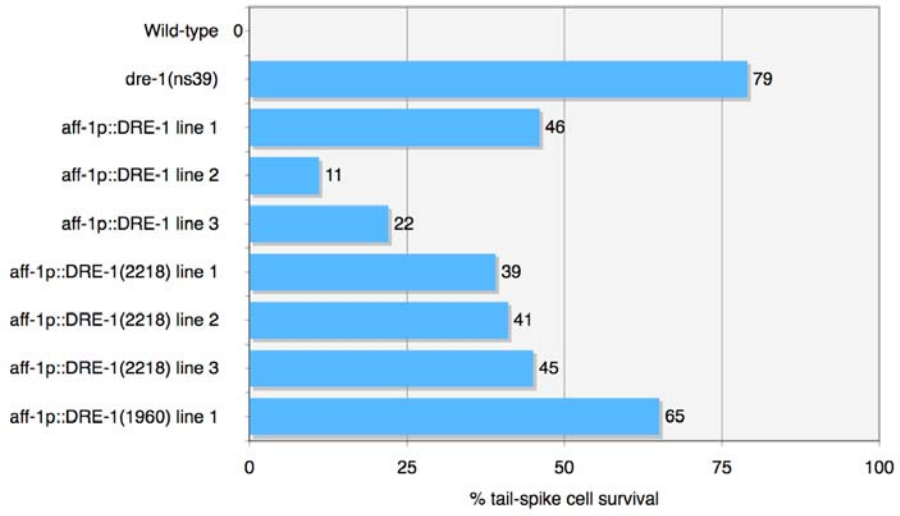

Fig. 33. Mutated forms of DRE-1/FBXO11 found in lymphomas have reduced ability to rescue the *dre-1(ns39)* tail-spike cell death defect. DRE-1(2218) corresponds to the Y560C mutation in FBXO11; DRE-1(1960) corresponds to the 256Stop mutation in FBXO11. All cDNAs were expressed using the *aff-1* promoter. Rescue of the *dre-1(ns39)* defect with the wild-type cDNA (*aff-1p*::DRE-1) is included for comparison. n>100 for each.

Overexpression of FBXO11 in human lymphoma lines induces apoptosis

Given the role of *dre-1* in apoptosis and the discovery of possible loss-of-function mutations in human lymphomas, it is possible that FBXO11 is a pro-apoptotic gene in human cells. If so, then its expression might induce death, a possibility that Lixin Rui, a post-doctoral fellow in Dr. Staudt's lab, investigated (all experiments described below involving human cells were performed by Dr. Rui). Transduction of a panel of lymphoma cell lines with a retrovirus expressing FBXO11 and GFP allowed the toxicity of FBXO11 to be evaluated via flow cytometry. While 11/18 lines showed no effect on viability over 8 days post-transduction, 7/18 exhibited a clear cell death phenotype (Fig. 34). Importantly, the three lines with deletions or mutations in FBXO11 – MedB1, Farage and OCI-Ly1 – showed a marked decrease in viability after FBXO11 expression, suggesting that loss of FBXO11 made these lines especially vulnerable to reintroduction of FBXO11.

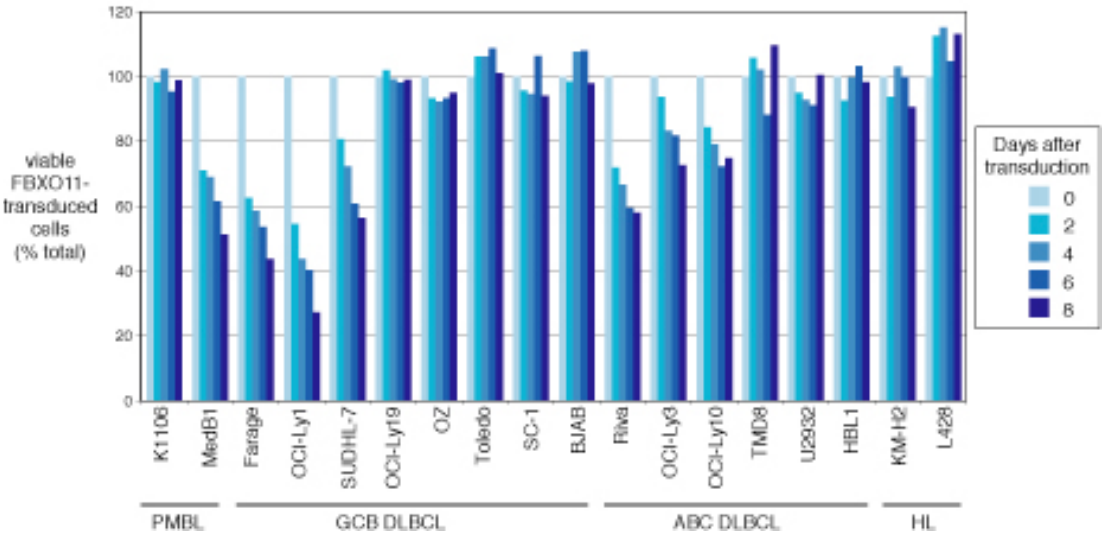

Fig. 34. Induction of FBXO11 expression kills certain lymphoma cell lines. Various DLBCL cell lines and two Hodgkin lymphoma cell lines, as indicated, were transduced with FBXO11 retrovirus. FBXO11-expressing cells were monitored by flow cytometry for a co-expressed GFP marker. The percentage of live GFP-positive cells for each time point was normalized to day 0. Lixin Rui and Lou Staudt, unpublished data.

This cell death phenotype was accompanied by hallmarks of apoptosis. Farage and MedB1, two of the lines most susceptible to FBXO11-induced death, showed an increase in cleaved PARP as well as active caspase-3 as assayed by flow cytometry (Fig. 35). VP16 expression was used as a positive control for induction of apoptosis.

FBXO11 induction did not affect the cell cycle in either cell line (Fig. 36).

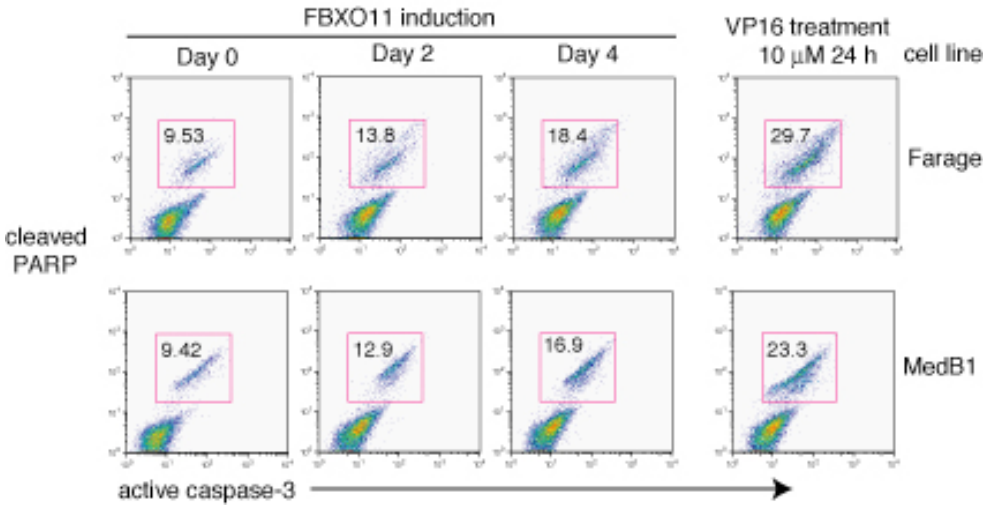

Fig. 35. FBXO11 expression induces apoptosis in lymphoma cell lines. Analysis of apoptosis with active caspase-3 and cleaved PARP in Farage and MedB1 cells expressing FBXO11 for the indicated times. Positive control cells were treated with VP16 as indicated times and concentrations. Lixin Rui and Lou Staudt, unpublished data.

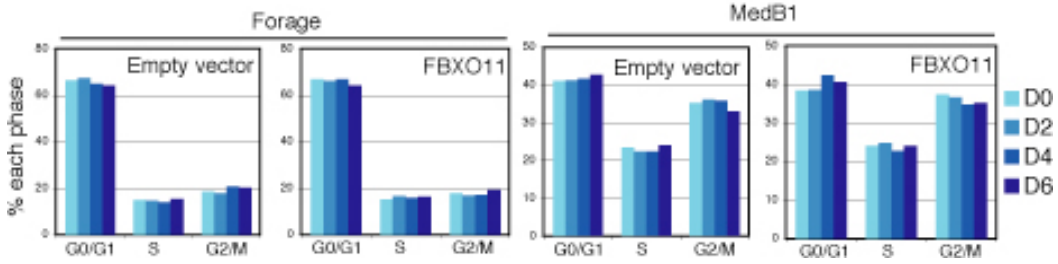

Fig. 36. FBXO11 expression does not affect the cell cycle. Flow cytometric analysis of the cell cycle in Farage and MedB1 cells induced for the expression of the FBXO11 for the indicated days. Empty vector served as a control. Lixin Rui and Lou Staudt, unpublished data.

FBXO11 kills lymphoma cells via degradation of BCL2

Because of the apparent connection between *dre-1* and *ced-9* in *C. elegans*, Dr. Rui tested whether induction of FBXO11 expression in Farage cells affected BCL2 levels. Remarkably, BCL2 levels decreased over the course of 4 days of FBXO11 expression, while no such change occurred in empty vector transduced cells (Fig. 37). This reduction in BCL2 protein level was evident both via immunoblot and flow cytometry.

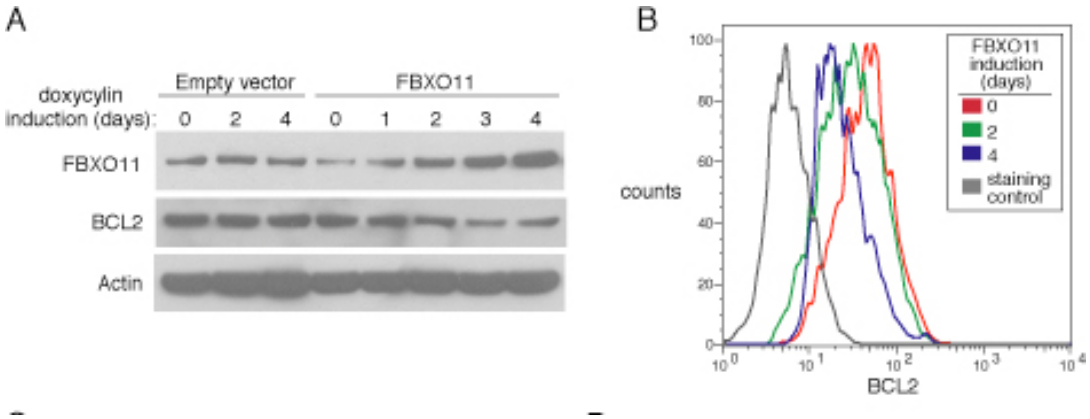

Fig. 37. BCL2 protein levels fall after FBXO11 expression.
(A) Immunobloting analysis of BCL2 levels after FBXO11 induction in Farage cells. The cells were transduced with FBXO11 or empty vector virus with puromycin selection marker and then induced for the expression of the FBXO11 for the indicated days.
(B) Flow cytometric analysis of the levels of BCL2 in the cells treated as in A. Lixin Rui and Lou Staudt, unpublished data.

Cell killing was significantly reduced when using mutant forms of FBXO11 derived from patient samples, the mouse mutant, and *C. elegans* mutants (Fig. 38). Furthermore, the potency of killing was well-correlated with the level of reduction of BCL2 protein detected by flow cytometry.

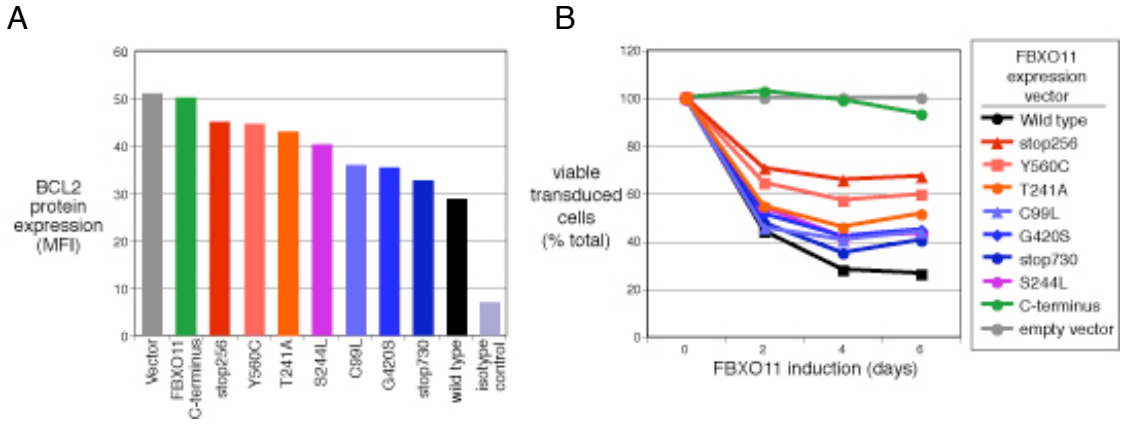

Fig. 38. The ability of FBXO11 to kill lymphoma cells and affect BCL2 levels is diminished in mutant forms of the protein.
(A) Farage cells were transduced with various mutant FBXO11 viruses and then expression was induced for 6 days. Shown is flow cytometric analysis of the levels of BCL2 protein.
(B) Farage cells were transduced with various FBXO11 retrovirus as indicated. FBXO11-expressing cells were monitored by flow cytometry for a co-expressed GFP marker. The percentage of live GFP-positive cells for each time point was normalized to day 0.
FBXO11 mutations: Y560C from OCI-Ly1 GCB cell line, T241A and stop256 (N-terminal 256 aa) from GCB patient samples. S244L from mouse ENU mutagenesis model. C99L, G420S and stop730 from *C. elegans* mutations. C-terminus (deletion of F-BOX domain) as a control. Lixin Rui and Lou Staudt, unpublished data.

To test whether overexpression of BCL2 could rescue the toxicity of FBXO11, HA-BCL2 was transduced into Farage cells and single cell clones expressing GFP and BCL2, or GFP and empty vector were selected. Those clones that expressed low levels of BCL2 (#9 and 10, as well as empty vector), but not those that expressed higher levels of BCL2 (#13, 15, 3, 11) were killed by FBXO11 induction (Fig. 39). Thus, a threshold level of BCL2 expression was required to rescue FBXO11 toxicity in Farage cells.

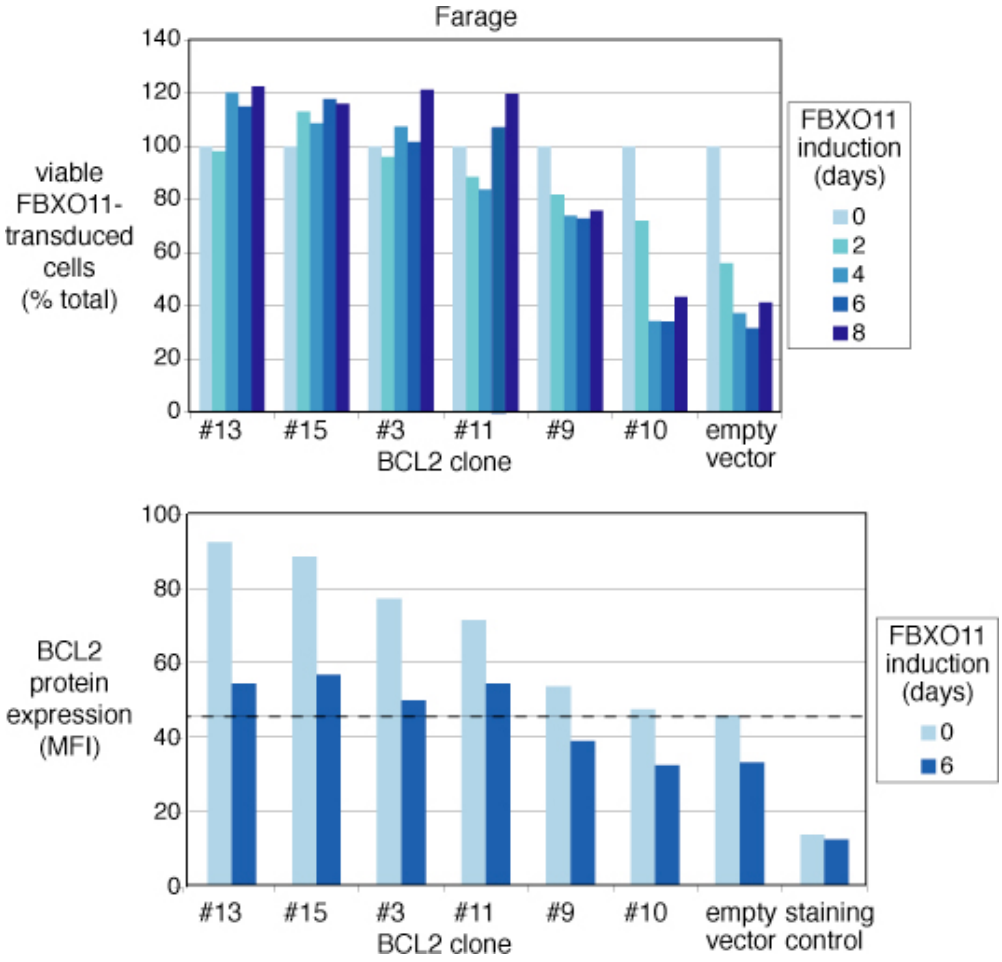

Fig. 39. Overexpression of BCL2 rescues the toxicity of FBXO11 to Farage cells.

Top panel: HA-BCL2 was transduced in Farage cells and single cell clones were obtained after hygromycin selection. These single cell clones were individually infected with FBXO11 retrovirus or empty vector with a GFP marker. Live FBXO11-expressing, GFP+ cells were monitored by flow cytometry over time following FBXO11 induction. Data were normalized today 0.

Bottom panel: Flow cytometric analysis of the levels of BCL2 protein in panel A samples after 6 days induction of FBXO11 compared to day 0. Lixin Rui and Lou Staudt, unpublished data.

The Farage line was selected for FBXO11 induction experiments because it completely lacks endogenous FBXO11 expression and is highly susceptible to killing upon FBXO11 reintroduction. However, to test whether FBXO11 and BCL2 interact physically, Dr. Rui used the Riva and OCI-Ly1 lines, which endogenously express FBXO11 and BCL2 but are also killed upon FBXO11 overexpression. Immunoprecipitation of lysates from Riva and OCI-Ly1 with an FBXO11 antibody but not a control antibody led to detection of BCL2 via immunoblotting (Fig. 40). Immunoprecipitation with the FBXO11 antibody from Farage serves as a negative control, since it expresses no FBXO11 but a large amount of BCL2.

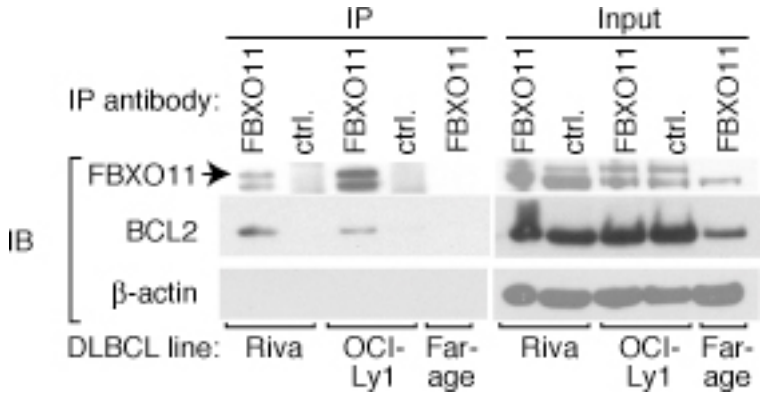

Fig. 40. FBXO11 and BCL2 interact in Riva and OCI-Ly1 cell lines. Immunoprecipitation with FBXO11 antibody but not a control antibody reveals an interaction between FBXO11 and BCL2. FBXO11 band is indicated by arrow. Lixin Rui and Lou Staudt, unpublished data.

The proteasome inhibitor PS-341 was used to test whether reduction of proteasome function would affect BCL2 immunoprecipitation with FBXO11. In both Riva and OCI-Ly1, there was an increase in BCL2 immunoprecipitated in the presence of PS-341, compared to no drug (Fig. 41, top panel). In the Riva cell line, this increase in BCL2 was evident over the 3 hour time course, as was a band corresponding to BCL2 in the anti-ubiquitin blot (Fig. 41, middle panel). The reciprocal experiment, in which BCL2 was immunoprecipitated in the presence of PS-341 and the lysate probed for FBXO11 showed a similar modest increase in FBXO11 over the 3 hour time course (Fig. 41, bottom panel). These results suggest that FBXO11 and BCL2 interact in these cell lines and their interaction is enhanced in the presence of the proteasome inhibitor PS-341.

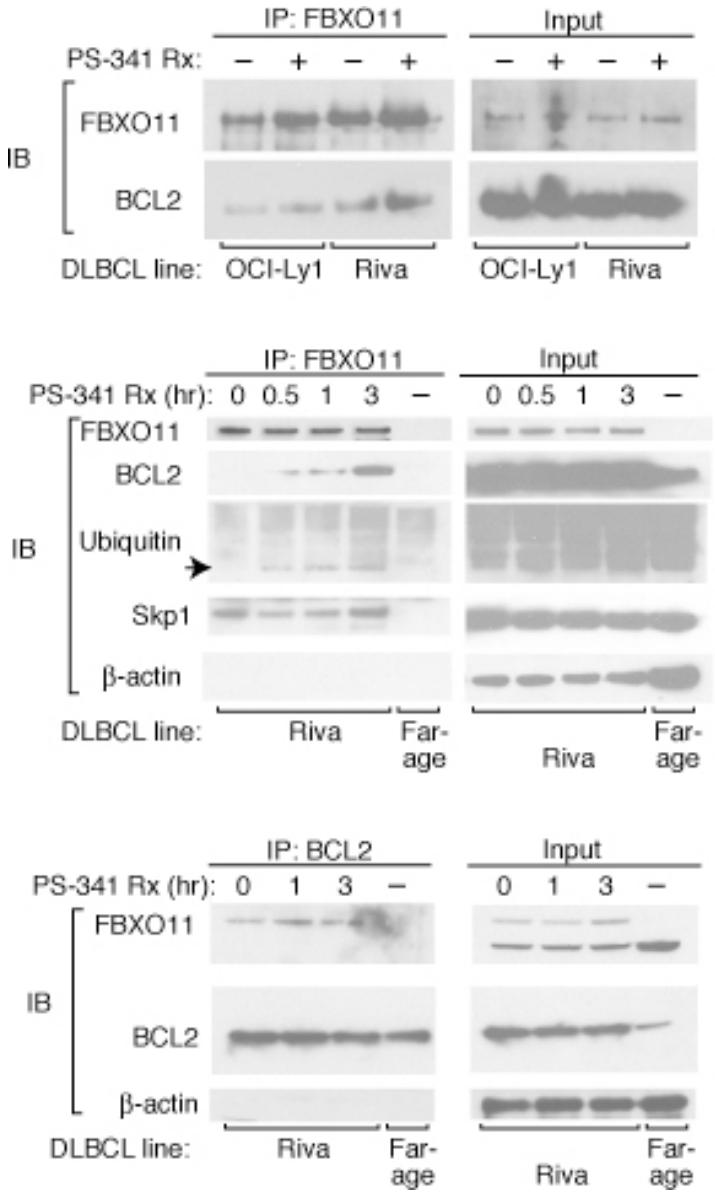

Fig. 41. Proteasome inhibition enhances BCL2 immunoprecipitation by FBXO11.

Cell lines were treated with PS-341 proteasome inhibitor for the indicated times and immunoprecipitated with antibodies against either FBXO11 or BCL2 and immunoblotted for the other. Lixin Rui and Lou Staudt, unpublished data.

5.3 Conclusions

Our results, in collaboration with Lou Staudt and Lixin Rui, suggest that FBXO11 is mutated in human lymphoma, and these mutations are loss-of-function mutations, both in the context of human cells and the tail-spike cell. Also, reintroduction of FBXO11 into human lymphoma cell lines that have lost the gene leads to their apoptotic death, and BCL2 overexpression can rescue this cell killing. FBXO11 interacts with BCL2 in lymphoma cells and leads to its degradation. Finally, we present evidence suggesting that DRE-1 and CED-9 physically interact in vitro, though we are unable to detect CED-9 protein in the tail-spike cell of *dre-1(ns39)* mutants by immunofluorescence.

Chapter 6: Characterization of global *ced-3* transcription and a mutant that affects *ced-3* transcription in the tail-spike cell

6.1 Background

Tail-spike cell death is unique in several ways, including the fact that it occurs a long time after the cell is born. Maurer et al. showed that a *ced-3pro::gfp* transcriptional reporter is activated just before the cell dies, suggesting that *ced-3* transcription is the trigger for the cell to die (Maurer et al., 2007). Furthermore, deletion of three small, conserved regions within the promoter abolished *ced-3pro::gfp* expression, showing that transcription factors must bind to the promoter to activate transcription. A forward genetic screen for mutants in which the *ced-3pro::gfp* construct fails to be activated identified three independent mutants, *ns114*, *ns115* and *ns90*. *ns114* and *ns115* mapped to the *pal-1* gene, a homeodomain transcription factor important in many cell fate decisions during development. Electrophoretic mobility shift assays showed that PAL-1 binds to the *ced-3* promoter to control tail-spike cell death, and the *pal-*

1(ns114) and *ns115* loss-of-function alleles block tail-spike cell death. These results established the importance of *ced-3* transcription in control of tail-spike cell death, but little was known about *ced-3* transcription in other cells. In addition, the *ns90* mutation, which completely blocks *ced-3* transcription in the tail-spike cell, remained uncloned. We set out to address these two issues.

6.2 Results

ced-3 is transcribed in most cells during development, including many that do not undergo programmed cell death

To create a transcriptional reporter that would include all relevant promoter sequences, we used the pJ40 plasmid, which has been shown to rescue the cell death defect of *ced-3* mutants (Yuan et al., 1993). Into this plasmid, which contains 7.6 kb of *ced-3* genomic DNA, we inserted the GFP sequence, followed by a stop codon. Thus, this construct encodes a protein containing the first 69 amino acids of CED-3 fused to GFP, followed by a long 3'UTR that includes the remainder of the *ced-3* gene and its own 3'UTR. Because such complicated mRNAs may be degraded by nonsense-mediated decay, we injected this construct into *smg-1(r861)* animals, which have been reported to allow expression of such transgenes (Wilkinson et al., 1994).

This reporter turned on ~100-150 minutes post-fertilization and expressed in most cells until the end of the comma stage of embryogenesis (Fig. 42). At this time, GFP was expressed in fewer and fewer cells, until hatching when GFP

was only reliably expressed in the tail-spike cell and occasionally in cells in the head (Fig. 42c). In addition, *ced-3* was also expressed in the male tail in L4 animals (Fig. 42d).

Having established that *ced-3* is transcribed in the tail-spike cell just before its death, we wondered whether a similar mechanism acted in other dying cells. To address this, we studied this reporter in *smg-1(r861); ced-3(n717)* animals, and found that there was no change in the expression pattern. If *ced-3* transcription is upregulated in all doomed cells just before their deaths, we would expect to see many cells in this strain that turned on the reporter just before their scheduled death but continued to express GFP after they survived inappropriately. Instead, we saw no evidence of these surviving, GFP-expressing cells, including in larvae in which cells die post-embryonically. Instead, we saw no significant GFP expression in larvae outside the tail-spike cell (Fig. 42e). We conclude that *ced-3* is transcribed in 100-150 minute embryos, and this mRNA or protein is inherited during development, when it can become activated in cells destined to die.

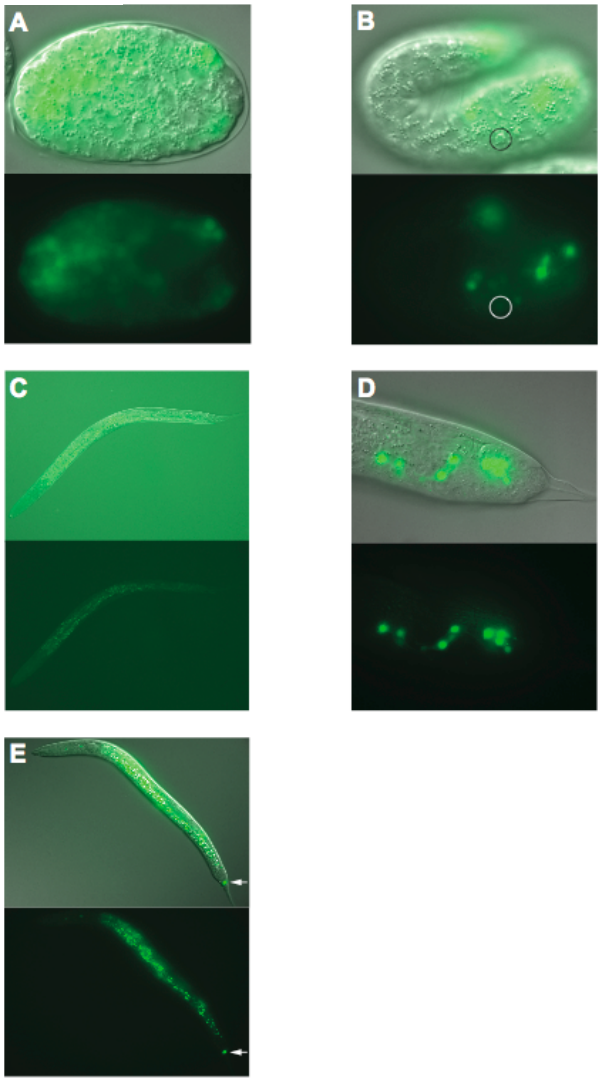

Fig. 42. *ced-3* is transcribed in many cells during developmental periods of cell death.
Top and bottom panels for each image are DIC+fluorescence and fluorescence-alone images, respectively. (A) Image of a *smg-1(r861)* embryo expressing a transgene consisting of the full rescuing (7.6 kb) *ced-3* genomic locus, into which GFP with a nuclear localization signal near the start codon was inserted. (B) Same as A. Notice cell corpse (circled) weakly expressing GFP. (C) A *smg-1(r861)* larva containing the same transgene as in A. Notice the absence of GFP expression. The observed fluorescence is caused by autofluorescence from gut granules. (D) A *smg-1(r861)* L4 male larva containing the same transgene as in A. Notice the bright expression in several cells in the tail. None of these cells is fated to die. (E) A *smg-1(r861); ced-3(n717)* larva containing the same transgene as in A. Notice the GFP expression in the tail-spike cell (arrows).

ns90 blocks *ced-3* transcription and apoptosis in the tail-spike cell

The *ns90* mutation was isolated from a screen for regulators of *ced-3* transcription in the tail-spike cell. *ced-3(n717); ced-3pro::gfp* animals, in which the tail-spike cell survives inappropriately in 100% of animals and expresses GFP, were mutagenized and F2 progeny in which *ced-3pro::gfp* was no longer present were sought. Three mutants were isolated from this screen, *ns114*, *ns115* and *ns90*. *ns114* and *ns115* were shown to be partial loss-of-function alleles of *pal-1*, in which the block in *ced-3* expression in the tail-spike cell was incomplete. *ns90*, on the other hand, produces a complete block in tail-spike cell *ced-3* transcription, such that the *nsIs25* transgene is off in 100% of animals. In addition, *ns90* is a semi-dominant mutant, as 96% of heterozygotes also lack *ced-3* transcription in the tail-spike cell.

Because of the complete block in *ced-3pro::gfp* expression in *ns90* mutants, we are unable to assess whether the mutation has an effect on tail-spike cell death or if it is instead never born. To circumvent this issue, we crossed the *ns90* mutation to the *ced-5(n1812)* background, in which apoptotic corpses persist inappropriately, allowing us to determine whether the cell has died. In *ns90; ced-5(n1812)* animals, a corpse is present in 41% of animals and absent in 59% (Fig. 43). These data suggest that the tail-spike cell is born and dies in less than half of animals, and in the remainder it is born and survives inappropriately, even though we are unable to visualize it with the *ced-3pro::gfp* reporter.

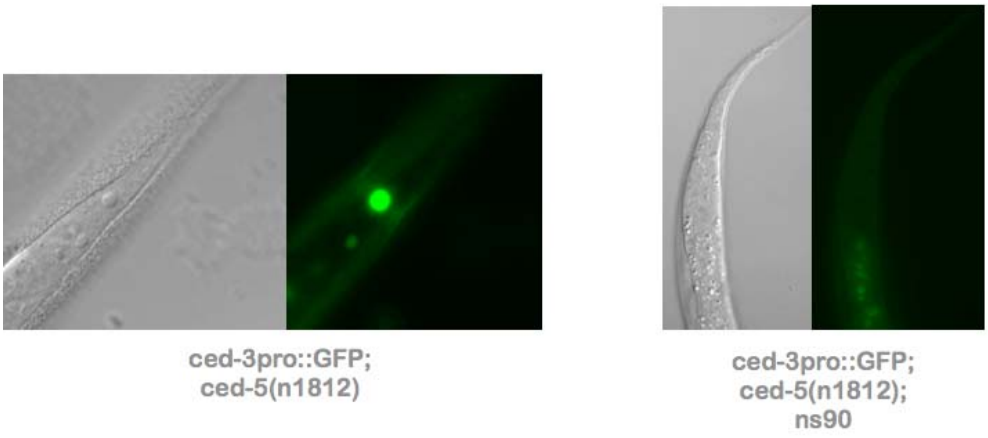

Fig. 43. The *ns90* mutation blocks tail-spike cell death in addition to *ced-3* transcription in the tail-spike cell.
Left: The tail of a *ced-5(n1812)* engulfment defective L1 larva in which the round, button-like tail-spike cell corpse is evident in DIC and fluorescence.
Right: The tail of an *ns90; ced-5(n1812)* larva in which no corpse is evident. 59% of animals of this genotype fail to display a corpse, suggesting that the *ns90* blocks tail-spike cell death in 59% of animals. All animals contain the *nsIs25* transgene as a marker for *ced-3* transcription in the tail-spike cell. n=30.

Because the *ns90* mutation appears to not only affect *ced-3* transcription but also tail-spike cell death, we set out to map this mutant via standard SNP-mapping techniques. However, because of the allele's dominance, we were forced to map the mutation based on the absence of the phenotype, i.e., picking recombinants in which the phenotype and mutation were lost. We were able to map the mutation to a 0.25 MU interval on Chromosome II between *T05C12.9* (0.75 MU) and *nfi-1* (0.5 MU). We sequenced several genes in this interval, including *lir-1*, *lir-2* and *lin-26*, and identified a mutation in *lin-26*. This mutation, a G to A change in the first zinc finger of the protein, is predicted to substitute an isoleucine for a methionine. Because of the difficulty of rescuing dominant mutations, we attempted to induce the *ns90* phenotype in wild-type animals by expressing the mutated form of *lin-26* in the tail-spike cell. This strategy proved unsuccessful, as 100% of *ced-3; nsIs25* animals carrying this transgene retained *ced-3pro::gfp* expression (n=30). Thus, we are unable to determine whether the mutation in *lin-26* is responsible for the *ns90* phenotype.

6.3 Conclusions

We have shown that the *ced-3* caspase is expressed in most cells during embryogenesis, including cells that do not undergo programmed cell death. This result is consistent with previous work showing that cells that do not undergo programmed cell death retain the pro-death activity of *ced-3*, although this killing activity is kept in check (Shaham and Horvitz, 1996b). Thus, it appears that *ced-*

3 is transcribed relatively early in embryogenesis, and either the transcript or protein is inherited during cell divisions until it is activated in cells fated for programmed cell death.

In addition, we showed that the *ns90* mutation, which was known to block *ced-3* transcription in the tail-spike cell, also prevents tail-spike cell death. We were unable to conclusively identify the gene relevant for the *ns90* phenotype, although we did identify a mutation in *lin-26*, a zinc-finger transcription factor (Labouesse et al., 1994). The mutation present in the *ns90* strain is a substitution in the first zinc-finger domain, which could disrupt binding of LIN-26 to the *ced-3* promoter. Indeed, while PAL-1 binds to the *ced-3* promoter in two defined domains, the transcription factor(s) that bind to the third domain shown by Maurer et al. to be important for *ced-3* transcription in the tail-spike cell remain unknown (Maurer et al., 2007). It is possible that LIN-26 is the relevant transcription factor, and the mutation we identified disrupts the ability to bind to this site. It is unclear why such a mutation would be dominant and so highly penetrant, although if LIN-26 acts in a dimer it could bind to and inactivate the wild-type form of the protein. Regardless, further work is required to elucidate the molecular basis of the *ns90* mutation.

Chapter 7: Discussion and Future Directions

Programmed cell death is a process crucial to the development of metazoans, and the genes underpinning this process are functionally important for development and disease, as well as fundamental to how life works. We have used the *C. elegans* tail-spike cell as a model for uncovering genes relevant to cell death, and these studies have revealed that a conserved F box protein, *dre-1*, is required for tail-spike cell death.

dre-1 acts within an SCF complex to regulate death, and represents a new mode of cell death control that bypasses *egl-1* to control caspase activation. *dre-1* requires *ced-9* for the majority of its function, suggesting that *dre-1* acts upstream of and/or in parallel to *ced-9*. Given that SCF complexes are known to induce ubiquitination and degradation of target proteins, and with our collaborators' results showing that FBXO11 and BCL2 interact physically, we favor a model in which the DRE-1 SCF complex inhibits CED-9 function directly, via ubiquitin-mediated proteolysis (Fig. 44). The *ced-9* epistasis results suggest

this model, but they also suggest that *dre-1* may function via another, *ced-9*-independent pathway. This is because in the absence of *ced-9* function (i.e., the *ced-9(n2812)* null mutation), the tail-spike cell still survives in 20% of animals. The only caveat to this result is that this strain contains three mutations, *dre-1(ns39)*, *ced-9(n2812)* and *ced-3(n2427)*, as well as the tail-spike cell integrated marker, making it possible that this highly unnatural state produces other effects that prevent tail-spike cell death (for example, *ced-4* expression could be affected). This result leads us to place *dre-1* upstream of *ced-9*, but also in parallel to it.

Our model also assumes that *rbx-1* and/or *-2* are part of the SCF complex that regulates tail-spike cell death. While we did not observe a tail-spike cell death phenotype for these genes, they are likely part of this complex, fulfilling the crucial E2 recruitment role. The lack of a discernable tail-spike cell phenotype in *rbx-1* or *-2* RNAi may be due to the difficulty of performing RNAi in the tail-spike cell: even in the *rrf-3* RNAi-sensitized background, knockdown of *ced-4*, which we would expect to give 100% survival based on the *ced-4(n1162)* allele, gives only 20% survival, illustrating that RNAi by the feeding method has a very weak effect in the tail-spike cell. Thus it is possible that the RNAi clones directed against *rbx-1* and *rbx-2* are unable to sufficiently knockdown the genes' function in order for us to observe an effect in the already weak tail-spike cell RNAi assay. Furthermore, feeding RNAi does not allow us to knockdown both genes simultaneously, so it is likely that knockdown of one gene results in redundant

compensation by the other. Thus, we are confident that DRE-1 acts in an SCF complex with SKR-1, CUL-1 and RBX-1/2.

Our model also suggests that DRE-1 acts directly on CED-9 to regulate cell death. As has been the case with many other E3 ligases, defining the target(s) of *dre-1* has been very difficult. We attempted to demonstrate an interaction between DRE-1 and CED-9 and found that they interact with weak affinity *in vitro*. That this interaction is difficult to detect may be due to the fact that we lack a *C. elegans* system in which DRE-1 and CED-9 are endogenously co-expressed, and instead we must ectopically express these proteins in *Drosophila* cells. If modifications are necessary to regulate this interaction, as is often the case in F box protein/substrate interactions, they may not be occur in this context. Also, because we lack specific antibodies appropriate for immunoprecipitation of DRE-1 and CED-9, we must use tagged forms of these proteins, which may affect their ability to interact. However, our results give evidence for a weak interaction of CED-9 and DRE-1.

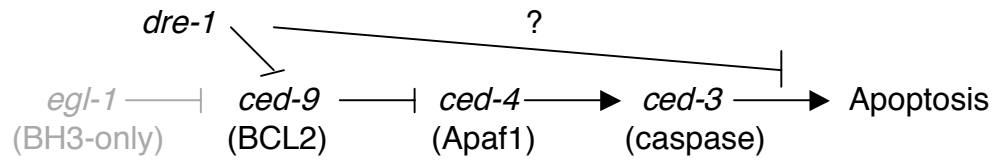

Fig. 44. A model for *dre-1's* role in tail-spike cell death.
Our results suggest that *dre-1*, in concert with its SCF complex partners (not shown), acts upstream of, or in parallel to *ced-9*, and may also act independently of *ced-9* to regulate tail-spike cell death.

What future experiments could allow us to identify the target(s) of DRE-1 in an unbiased manner? First, a genetic screen for dominant mutations that prevent tail-spike cell death could be informative. Indeed, we attempted such a screen, and isolated one mutant, *ns312*, but were unable to clone it, as it appeared to map to two separate loci and was not strongly dominant. However, a more exhaustive screen of this variety could isolate a dominant-negative form of an anti-apoptotic regulator, as *ced-9(n1950)* was isolated from screens for inappropriate cell survival. A dominant mutant might represent a mutation that prevents *dre-1*'s target from interacting with the SCF complex and thus from being ubiquitinated. In that case, the anti-apoptotic activity of the target protein would persist and prevent the tail-spike cell from dying. The major caveat to this screen is that such a mutant may not exist: there may not be a mutation that

prevents binding of this anti-apoptotic protein to the *dre-1* SCF complex while also leaving its anti-apoptotic function intact. Indeed, our failed attempts at isolating such a mutant provide support to this idea, although our screen was not exhaustive and further attempts could prove fruitful here.

A related experiment could address whether CED-9 is the relevant target of DRE-1 in tail-spike cell death. Wild-type and un-ubiquitinatable *ced-9* could be expressed in the tail-spike cell, and assayed for their ability to prevent tail-spike cell death. If ubiquitin-mediated destruction or inhibition is necessary for tail-spike cell death, then the un-ubiquitinatable form would be expected to prevent death at a higher rate than the wild-type form. This experiment is difficult, however, for two reasons. First, there are 13 lysines in CED-9, and it is impossible to know, *a priore*, which are relevant. It is intriguing, however, that CED-9, BCL2 and many of their homologues share a terminal lysine residue. Second, we know that there is at least one form of CED-9 that dominantly prevents cell death, *n1950*, through its *egl-1*-related interaction. While this interaction plays a minor role in the tail-spike cell, it might complicate the interpretation of the results. Third and most importantly, the level of expression of wild-type and mutant forms of CED-9 are crucial determinants in this experiment. *C. elegans* transgenics are known to vary significantly in the copy numbers of the introduced genes. If either the wild-type or mutant forms of CED-9 were expressed at a very high level, the amount of tail-spike cell death in the strain could be affected, as in either case, high expression of an anti-apoptotic

protein should prevent death. Excess tail-spike cell survival due to high expression of CED-9 would have to be distinguished from physiologic expression of a mutant form that accumulates due to lack of proteasome-induced turnover.

A second avenue toward identifying the target of DRE-1 would be to clone more mutants from the screen that yielded the *dre-1(ns39)* mutant. Because many F box protein-substrate interactions require phosphorylation or other modification for efficient binding, it is likely that there are other genes involved in *dre-1*'s pro-apoptotic function in the tail-spike cell. Indeed, another mutant, *ns40*, fails to complement *dre-1* and does not have a global cell death defect, suggesting that this may be an interesting mutant. Also, the screen that isolated *ns39* and *ns40* is not saturated, so more interesting mutants may be available after further screening.

Third, DRE-1 binding partners could be isolated with a biochemical screen. For example, a tagged form of DRE-1 could be used to rescue the tail-spike cell death defect and then an antibody against the tag could be used to isolate DRE-1 and proteins bound to it. Knowing that the tagged form rescued the death defect would assure that full *dre-1* activity was present in the ectopically-expressed strain. The protein isolation would ideally be done in embryos, when *dre-1* acts in the tail-spike cell; otherwise, *dre-1* targets relevant to heterochronic or early development phenotypes might be isolated instead. Not only is this a difficult experiment because of the inherent difficulty in performing a biochemical screen, but also because the tail-spike cell is one of ~1000 cells in

the animal, and thus the relevant interaction might be below the level of detection.

Finally, to investigate further whether CED-9 is the target of DRE-1, biochemical isolation of CED-9 protein from *C. elegans* embryos followed by biochemical analysis could be done. If CED-9 is polyubiquitinated, phosphorylated, or otherwise modified, these modifications might be discernible by mass spectrometry. While this may be less successful in whole *C. elegans* embryos, as the tail-spike cell is one of many cells, it might be more successful in human lymphoma cells susceptible to FBXO11-induced killing. Identification of the residues relevant for ubiquitination or other modification would allow those amino acids to be specifically targeted for mutagenesis in further studies.

While we have focused on the cell death-related target(s) of DRE-1, it would also be interesting to understand what are the other DRE-1 targets that govern other developmental processes. For example, *dre-1(null)* mutants die during embryogenesis due to severe patterning defects that are unrelated to cell death. In addition, Fielenbach et al. described a role for *dre-1* in heterochronic phenotypes in larvae (Fielenbach et al., 2007). While these functions are clearly separable from *dre-1*'s cell death function (that the *ns39* mutant is viable but has a strong tail-spike cell death defect demonstrates this), they may be in some way shed light on the apoptotic role. A relatively simple screen would be for suppressors of the lethality of a *dre-1(null)* mutation.

We showed that most *aff-1* mutant animals have a forked tail as L1s, and

this defect is likely to be due to tail-spike cell non-fusion because fusion of hyp10, the cell that makes up the tail tip, is governed by *eff-1*. We have not, however, formally proved this, as it is possible that the *aff-1* mutation affects tail-tip morphogenesis via another cell, despite the fact that *aff-1* is expressed in the tail-spike cell but not hyp10. To formally prove that tail-spike cell fusion must occur for proper tail-tip morphogenesis, we would have to rescue the *aff-1* mutation in the tail-spike cell only. However, no promoter is known that expresses specifically in the tail-spike cell at an early stage in development.

Our results also suggest that the tail-spike cell process is vital for hyp10 morphogenesis, and when the cell does not fuse, two processes are produced which direct formation of a forked tail, instead of a normal one. To more directly address this hypothesis, we could ablate either the developing tail-spike cell soon after its birth, or the process as it has just begun to form. We would expect that in either case, hyp10 would be unable to properly form a tail-tip, a defect that might manifest itself as a blunted tail. The difficulty with this experiment is that ablations would have to be performed in 3-fold embryos in which the animals are able to roll within the eggshell. Thus, it would be difficult to ablate such a small cell, or, better, its even smaller process, in a moving target.

When we recognized that *dre-1* is a conserved apoptotic regulator, we wondered whether its cell death role was conserved, and whether it might act as a tumor suppressor in human cancer. Our collaborators at the National Cancer

Institute, Lou Staudt and Lixin Rui, identified human lymphoma cell lines and patient samples with deletions and mutations in the FBXO11 gene consistent with the idea that FBXO11 controls apoptosis in human lymphoma (that tail-spike cell death is governed by two suppressors of human cancer, *pal-1*/Cdx2 and *dre-1*/FBXO11, is truly remarkable). They went on to show that FBXO11 expression in the cells that had deleted it caused their death, suggesting that, because of the genetic wiring of these particular cell lines, FBXO11 is especially toxic. In addition, they were able to show that FBXO11 and BCL2 interact in the cells in which both are endogenously expressed, and that BCL2 levels fall upon FBXO11 expression.

An ENU-induced mutant in FBXO11 has been described, the so-called Jeff mouse, which is likely a hypomorphic mutation that leads to perinatal lethality in homozygotes. Because these mice do not survive beyond a few hours after birth, we cannot test whether they are cancer-prone. However, as heterozygotes these animals are viable and show only an inner ear defect. To address whether FBXO11 plays a role in tumor suppression in mice, these heterozygotes could be monitored for spontaneous tumor development, although the Jf/+ reduction of function may not be a strong enough FBXO11 defect to induce tumor formation. In that case, Jf/+ heterozygotes could be crossed to one of many tumor-prone mouse models, such as the Eμ-myc model. In these mice, the myc oncogene is driven by the immunoglobulin heavy chain enhancer, and nearly all mice containing this transgene develop lymphomas at a young age. If FBXO11 is

involved in B cell death, Jf/+ Eμ-myc mice might develop tumors at an earlier age, or their tumors might be more virulent

Another interesting experiment would be to conditionally inactivate FBXO11 in B cells, replacing the coding sequence in B cells with GFP via the Cre-lox or other related system. This would allow monitoring of B cell development in the absence of FBXO11, which might elucidate the step at which the gene is acting. Simultaneously, it would give information about when during B cell development FBXO11 is normally expressed. Because B cells may undergo apoptosis at many steps during their maturation, from early stages when they must successfully rearrange their immunoglobulin loci to form a competent B cell receptor, to later stages when they may be deleted based on the affinity of their receptor for self- and non-self-antigen. We would predict, based on the mutations found in DLBCL, that FBXO11 is more likely to act in later B cell development, as these tumors express gene signatures seen in later stage B cells. A detailed examination of FBXO11 expression in normal B cells with an anti-FBXO11 antibody would further our understanding of its role in B cell development.

A related experiment that would help to understand the role of FBXO11 in vertebrate systems would be the creation of a GFP knock-in mouse to replace the FBXO11 locus in all cells. This would allow the FBXO11 expression pattern to be studied in detail during development, along with the null phenotype. We do not know how far these mice would develop, but if they survived long enough in

embryogenesis, we would learn in which tissues FBXO11 is expressed with more accuracy than has been reported via immunostaining.

The Jf/Jf mouse has been reported to possess craniofacial abnormalities and cleft palate, and shows reduced staining of cleaved caspase-3 in the developing palate (Tateossian et al., 2009). Intriguingly, Apaf-1 mutants were also reported with facial deformities and cleft palate (Cecconi et al., 1998). While there are many mouse mutants with these phenotypes, it is tempting to think that both the FBXO11 and Apaf-1 defects are cell death-related defects. To address this question, it would be informative to stain the developing palates of Jf/Jf mice for Apaf-1 and BCL2, as well as Apaf-1(null) mice for FBXO11 expression; perhaps the expression of one depends on the presence of the other. Also, developing palates of wild-type mice could be stained for these proteins, as they may be expressed in a subset of cells that must undergo programmed cell death for a normal palate to be formed.

Finally, because of the connection between FBXO11 and BCL2, and because BCL2 is expressed in tissues outside B cells and has been implicated in many other cancers, sequencing of the FBXO11 locus in other tumor types could be informative. While Rui and Staudt found FBXO11 mutation in 5% of germinal center-like DLBCLs, it is possible that the gene is mutated in other tumor types at a higher rate. In addition, Tateossian et al. reported that FBXO11 is expressed in many tissues of the mouse, including lung, brain, bone marrow and kidney. If the human FBXO11 expression pattern is similar, then FBXO11 may have a role in

the development of these tissues and may also have tumor suppressive activity in these tissues. With the ongoing Cancer Genome Atlas and other deep sequencing projects in progress, we may learn of FBXO11 mutations in other cancers.

Chapter 8: Materials and Methods

Strains

All strains were maintained at 20°C on NGM agar with OP50 bacteria. The wild-type strain was N2 Bristol. The following strains were used:

LGI: *mir-71(n4115), mir-2(n4108), lin-28(n719), skr-1(sm151, ok1696)*

LGII: *aff-1(tm2214), eff-1(hy40), ns90, lin-29(n333), lin-4(e912), rrf-3(pk1426)*

LGIII: *ced-4(n1162, n), ced-9(n2812, n1950), pal-1(ns114, ns115), cul-1(e1756)*

LGIV: *ced-3(n717, n2427, n2436, ns38), ced-5(n1812)*

LGV: *dre-1(ns39, dh99, dh279, gk857), egl-1(n1084n3082), lin-46(ma164)*

LGX: *nsIs25*

Plasmid construction

For the *dre-1* transcriptional reporter, 4 kb of genomic DNA upstream of *dre-1* exon 2 was amplified by PCR with SalI and BamHI sites incorporated into the primers and the resulting amplicon was ligated into pPD95-69. For *dre-1* cDNA

rescue constructs, the *dre-1* cDNA was amplified from purified mixed stage C. elegans cDNA and ligated via TOPO cloning into the pCRII-TOPO vector (Invitrogen). From this template, the *dre-1* cDNA was amplified with primers including SpeI and SalI sites, and the resulting amplicon ligated into pBluescript. The *dre-1* 3'UTR was amplified by PCR from genomic DNA and ligated with SalI and ApaI sites downstream of the *dre-1* cDNA in this plasmid. Finally, various promoters were amplified from genomic DNA and ligated using NotI and SpeI sites: 4.4 kb of genomic DNA upstream of the aff-1 ATG was used for aff-1p::DRE-1 plasmids; 730 bp of genomic DNA upstream of the dpy-30 ATG was used for dpy-30p::DRE-1 plasmids. *dre-1* mutations were introduced into the cDNA by PCR. Briefly, two anti-parallel primers containing the desired mutation were used along with primers complementary to the beginning and end of the cDNA to produce two PCR products that included the desired mutation. These products were then used as the template for a third PCR in which primers complementary to the beginning and end of the cDNA were used. The resulting amplicon was ligated into the plasmid described above in place of the wild-type cDNA. This strategy was used to create the aff-1p::DRE-1(2218) and aff-1p::DRE-1(1960) mutant forms of the cDNA. *Drosophila* S2 cell culture transfections were done with the relevant cDNA cloned into the pAC5.1 vector.

Transgenic strains

All rescue experiments were performed using 5 ng/ul rescuing plasmid or fosmid + 15 ng/ul coelomocyte::dsRed coinjection marker (a gift from Carl Procko) + 80 ng/ul pBluescript. Fluorescent reporters were injected at 25 ng/ul with pRF4 rol-6 plasmid.

Immunostaining with anti-CED-9 antibodies

Immunostaining was attempted as described by Finney and Ruvkun (1990), as well as with the freeze-crack method of Janet Duerr. Goat anti-CED-9 antibodies were used at 1:50-1:200 concentrations.

***Drosophila* S2 cell culture**

S2 cells were grown in Shields and Sang M3 insect medium with 10% FBS and penn-strep at 50 units/ml at 25°C. For transfections, 2 million cells in 2 ml culture medium were split into 6 well plates, and the following day cells were transfected with 1 ug plasmid DNA + 8 ul Fugene HD Transfection Reagent (Roche). Analysis was performed 3 days later.

Immunoprecipitation

2-10 ml transfected cells were pelleted by centrifugation and washed with 1 ml cold PBS. Cells were lysed in 500 ul NP-40 lysis buffer with 250 mM NaCl for 1 hour at 4°C. myc::CED-9 was immunoprecipitated with rabbit polyclonal anti-myc

(AbCam) + Dynabeads (Invitrogen) for 30 min at 20°C. The complexes were isolated and washed according to the manufacturer's directions and analyzed by SDS-PAGE.

RNA interference

HT1114 E. coli carrying the relevant RNAi plasmid were grown overnight at 37°C in LB+ampicillin. Bacteria were plated on NGM+IPTG+carbenicillin plates and incubated at 37°C with the lids askew for 3 hours to dry, followed by upside-down overnight to grow. The following day, *rrf-3(pk1426);nsIs25* young adult hermaphrodites were placed on the lawn. For the next two days, L1 progeny were scored for tail-spike cell survival under a compound fluorescence microscope.

References

Abida, W. M., Nikolaev, A., Zhao, W., Zhang, W., and Gu, W. (2007). FBXO11 promotes the Neddylation of p53 and inhibits its transcriptional activity. J Biol Chem *282*, 1797-1804.

Akiyama, T., Bouillet, P., Miyazaki, T., Kadono, Y., Chikuda, H., Chung, U. I., Fukuda, A., Hikita, A., Seto, H., Okada, T.*, et al.* (2003). Regulation of osteoclast apoptosis by ubiquitylation of proapoptotic BH3-only Bcl-2 family member Bim. Embo J *22*, 6653-6664.

Aoki, K., Tamai, Y., Horiike, S., Oshima, M., and Taketo, M. M. (2003). Colonic polyposis caused by mTOR-mediated chromosomal instability in Apc+/Delta716 Cdx2+/- compound mutant mice. Nat Genet *35*, 323-330.

Arama, E., Agapite, J., and Steller, H. (2003). Caspase activity and a specific cytochrome C are required for sperm differentiation in Drosophila. Dev Cell *4*, 687-697.

Arama, E., Bader, M., Rieckhof, G. E., and Steller, H. (2007). A ubiquitin ligase complex regulates caspase activation during sperm differentiation in Drosophila. PLoS Biol *5*, e251.

Bader, M., Arama, E., and Steller, H. (2010). A novel F-box protein is required for caspase activation during cellular remodeling in Drosophila. Development *137*, 1679-1688.

Bartke, T., Pohl, C., Pyrowolakis, G., and Jentsch, S. (2004). Dual role of BRUCE as an antiapoptotic IAP and a chimeric E2/E3 ubiquitin ligase. Mol Cell *14*, 801-811.

Bech-Otschir, D., Helfrich, A., Enenkel, C., Consiglieri, G., Seeger, M., Holzhutter, H. G., Dahlmann, B., and Kloetzel, P. M. (2009). Polyubiquitin substrates allosterically activate their own degradation by the 26S proteasome. Nat Struct Mol Biol *16*, 219-225.

Besche, H. C., Peth, A., and Goldberg, A. L. (2009). Getting to first base in proteasome assembly. Cell *138*, 25-28.

Bonhomme, C., Duluc, I., Martin, E., Chawengsaksophak, K., Chenard, M.-P., Kedinger, M., Beck, F., Freund, J.-N., and Domon-Dell, C. (2003). The Cdx2 homeobox gene has a tumour suppressor function in the distal colon in addition to a homeotic role during gut development. Gut *52*, 1465-1471.

Breitschopf, K., Haendeler, J., Malchow, P., Zeiher, A. M., and Dimmeler, S. (2000). Posttranslational modification of Bcl-2 facilitates its proteasome-dependent degradation: molecular characterization of the involved signaling pathway. Mol Cell Biol *20*, 1886-1896.

Cecconi, F., Alvarez-Bolado, G., Meyer, B. I., Roth, K. A., and Gruss, P. (1998). Apaf1 (CED-4 homolog) regulates programmed cell death in mammalian development. Cell *94*, 727-737.

Chai, J., Yan, N., Huh, J. R., Wu, J. W., Li, W., Hay, B. A., and Shi, Y. (2003). Molecular mechanism of Reaper-Grim-Hid-mediated suppression of DIAP1-dependent Dronc ubiquitination. Nat Struct Biol *10*, 892-898.

Conradt, B., and Horvitz, H. R. (1998). The C. elegans protein EGL-1 is required for programmed cell death and interacts with the Bcl-2-like protein CED-9. Cell *93*, 519-529.

Cook, J. R., Lee, J.-H., Yang, Z.-H., Krause, C. D., Herth, N., Hoffmann, R., and Pestka, S. (2006). FBXO11/PRMT9, a new protein arginine methyltransferase, symmetrically dimethylates arginine residues. Biochem Biophys Res Commun *342*, 472-481.

Deshaies, R. J., and Joazeiro, C. A. (2009). RING domain E3 ubiquitin ligases. Annu Rev Biochem *78*, 399-434.

Deveraux, Q. L., Takahashi, R., Salvesen, G. S., and Reed, J. C. (1997). X-linked IAP is a direct inhibitor of cell-death proteases. Nature *388*, 300-304.

Dimmeler, S., Breitschopf, K., Haendeler, J., and Zeiher, A. M. (1999). Dephosphorylation targets Bcl-2 for ubiquitin-dependent degradation: a link between the apoptosome and the proteasome pathway. J Exp Med *189*, 1815-1822.

Ditzel, M., Broemer, M., Tenev, T., Bolduc, C., Lee, T. V., Rigbolt, K. T., Elliott, R., Zvelebil, M., Blagoev, B., Bergmann, A., and Meier, P. (2008). Inactivation of effector caspases through nondegradative polyubiquitylation. Mol Cell *32*, 540-553.

Ditzel, M., Wilson, R., Tenev, T., Zachariou, A., Paul, A., Deas, E., and Meier, P. (2003). Degradation of DIAP1 by the N-end rule pathway is essential for regulating apoptosis. Nat Cell Biol *5*, 467-473.

Ellis, H. M., and Horvitz, H. R. (1986). Genetic control of programmed cell death in the nematode C. elegans. Cell *44*, 817-829.

Feldman, R. M., Correll, C. C., Kaplan, K. B., and Deshaies, R. J. (1997). A complex of Cdc4p, Skp1p, and Cdc53p/cullin catalyzes ubiquitination of the phosphorylated CDK inhibitor Sic1p. Cell *91*, 221-230.

Fielenbach, N., Guardavaccaro, D., Neubert, K., Chan, T., Li, D., Feng, Q., Hutter, H., Pagano, M., and Antebi, A. (2007). DRE-1: an evolutionarily conserved F box protein that regulates C. elegans developmental age. Dev Cell *12*, 443-455.

Glucksmann, A. (1951). Cell deaths in normal vertebrate ontogeny. Biol Rev *29*, 59-86.

Goyal, L., McCall, K., Agapite, J., Hartwieg, E., and Steller, H. (2000). Induction of apoptosis by Drosophila reaper, hid and grim through inhibition of IAP function. Embo J *19*, 589-597.

Groll, M., Bajorek, M., Kohler, A., Moroder, L., Rubin, D. M., Huber, R., Glickman, M. H., and Finley, D. (2000). A gated channel into the proteasome core particle. Nat Struct Biol *7*, 1062-1067.

Gumienny, T. L., Lambie, E., Hartwieg, E., Horvitz, H. R., and Hengartner, M. O. (1999). Genetic control of programmed cell death in the Caenorhabditis elegans hermaphrodite germline. Development *126*, 1011-1022.

Hanahan, D., and Weinberg, R. A. (2000). The hallmarks of cancer. Cell *100*, 57-70.

Hao, B., Oehlmann, S., Sowa, M. E., Harper, J. W., and Pavletich, N. P. (2007). Structure of a Fbw7-Skp1-cyclin E complex: multisite-phosphorylated substrate recognition by SCF ubiquitin ligases. Mol Cell *26*, 131-143.

Hao, Y., Sekine, K., Kawabata, A., Nakamura, H., Ishioka, T., Ohata, H., Katayama, R., Hashimoto, C., Zhang, X., Noda, T.*, et al.* (2004). Apollon

ubiquitinates SMAC and caspase-9, and has an essential cytoprotection function. Nat Cell Biol *6*, 849-860.

Hardisty, R. E., Erven, A., Logan, K., Morse, S., Guionaud, S., Sancho-Oliver, S., Hunter, A. J., Brown, S. D. M., and Steel, K. P. (2003). The deaf mouse mutant Jeff (Jf) is a single gene model of otitis media. J Assoc Res Otolaryngol *4*, 130-138.

Hardisty-Hughes, R. E., Tateossian, H., Morse, S. A., Romero, M. R., Middleton, A., Tymowska-Lalanne, Z., Hunter, A. J., Cheeseman, M., and Brown, S. D. M. (2006). A mutation in the F-box gene, Fbxo11, causes otitis media in the Jeff mouse. Hum Mol Genet *15*, 3273-3279.

Hengartner, M. O., Ellis, R. E., and Horvitz, H. R. (1992). Caenorhabditis elegans gene ced-9 protects cells from programmed cell death. Nature *356*, 494-499.

Hengartner, M. O., and Horvitz, H. R. (1994). Activation of C. elegans cell death protein CED-9 by an amino-acid substitution in a domain conserved in Bcl-2. Nature *369*, 318-320.

Hicke, L., Schubert, H. L., and Hill, C. P. (2005). Ubiquitin-binding domains. Nat Rev Mol Cell Biol *6*, 610-621.

Hoeller, D., Hecker, C. M., and Dikic, I. (2006). Ubiquitin and ubiquitin-like proteins in cancer pathogenesis. Nat Rev Cancer *6*, 776-788.

Killian, D. J., Harvey, E., Johnson, P., Otori, M., Mitani, S., and Xue, D. (2008). SKR-1, a homolog of Skp1 and a member of the SCF(SEL-10) complex, regulates sex-determination and LIN-12/Notch signaling in C. elegans. Dev Biol *322*, 322-331.

Kraus, B., Pohlschmidt, M., Leung, A. L., Germino, G. G., Snarey, A., Schneider, M. C., Reeders, S. T., and Frischauf, A. M. (1994). A novel cyclin gene (CCNF) in the region of the polycystic kidney disease gene (PKD1). Genomics *24*, 27-33.

Kun, A., Santos, M., and Szathmáry, E. (2005). Real ribozymes suggest a relaxed error threshold. Nat Genet *37*, 1008-1011.

Labouesse, M., Sookhareea, S., and Horvitz, H. R. (1994). The Caenorhabditis elegans gene lin-26 is required to specify the fates of hypodermal cells and encodes a presumptive zinc-finger transcription factor. Development *120*, 2359-2368.

Le Poole, I. C., Sarangarajan, R., Zhao, Y., Stennett, L. S., Brown, T. L., Sheth, P., Miki, T., and Boissy, R. E. (2001). 'VIT1', a novel gene associated with vitiligo. Pigment Cell Res *14*, 475-484.

Lenz, G., and Staudt, L. M. (2010). Aggressive lymphomas. N Engl J Med *362*, 1417-1429.

Ley, R., Balmanno, K., Hadfield, K., Weston, C., and Cook, S. J. (2003). Activation of the ERK1/2 signaling pathway promotes phosphorylation and proteasome-dependent degradation of the BH3-only protein, Bim. J Biol Chem *278*, 18811-18816.

Li, S., Armstrong, C. M., Bertin, N., Ge, H., Milstein, S., Boxem, M., Vidalain, P.-O., Han, J.-D. J., Chesneau, A., Hao, T.*, et al.* (2004). A map of the interactome network of the metazoan C. elegans. Science *303*, 540-543.

Li, X., and Demartino, G. N. (2009). Variably modulated gating of the 26S proteasome by ATP and polyubiquitin. Biochem J *421*, 397-404.

Lin, S. S., Bassik, M. C., Suh, H., Nishino, M., Arroyo, J. D., Hahn, W. C., Korsmeyer, S. J., and Roberts, T. M. (2006). PP2A regulates BCL-2 phosphorylation and proteasome-mediated degradation at the endoplasmic reticulum. J Biol Chem *281*, 23003-23012.

Lisi, S., Mazzon, I., and White, K. (2000). Diverse domains of THREAD/DIAP1 are required to inhibit apoptosis induced by REAPER and HID in Drosophila. Genetics *154*, 669-678.

Maurer, C. W., Chiorazzi, M., and Shaham, S. (2007). Timing of the onset of a developmental cell death is controlled by transcriptional induction of the C. elegans ced-3 caspase-encoding gene. Development *134*, 1357-1368.

Meier, P., Finch, A., and Evan, G. (2000). Apoptosis in development. Nature *407*, 796-801.

Mohler, W. A., Shemer, G., del Campo, J. J., Valansi, C., Opoku-Serebuoh, E., Scranton, V., Assaf, N., White, J. G., and Podbilewicz, B. (2002). The type I membrane protein EFF-1 is essential for developmental cell fusion. Dev Cell *2*, 355-362.

Mukhopadhyay, S., Lu, Y., Qin, H., Lanjuin, A., Shaham, S., and Sengupta, P. (2007). Distinct IFT mechanisms contribute to the generation of ciliary structural diversity in C. elegans. EMBO J *26*, 2966-2980.

Nayak, S., Santiago, F. E., Jin, H., Lin, D., Schedl, T., and Kipreos, E. T. (2002). The Caenorhabditis elegans Skp1-related gene family: diverse functions in cell proliferation, morphogenesis, and meiosis. Curr Biol *12*, 277-287.

Peth, A., Besche, H. C., and Goldberg, A. L. (2009). Ubiquitinated proteins activate the proteasome by binding to Usp14/Ubp6, which causes 20S gate opening. Mol Cell *36*, 794-804.

Podbilewicz, B., Leikina, E., Sapir, A., Valansi, C., Suissa, M., Shemer, G., and Chernomordik, L. V. (2006). The C. elegans developmental fusogen EFF-1 mediates homotypic fusion in heterologous cells and in vivo. Dev Cell *11*, 471-481.

Ryoo, H. D., Bergmann, A., Gonen, H., Ciechanover, A., and Steller, H. (2002). Regulation of Drosophila IAP1 degradation and apoptosis by reaper and ubcD1. Nat Cell Biol *4*, 432-438.

Ryoo, H. D., Gorenc, T., and Steller, H. (2004). Apoptotic cells can induce compensatory cell proliferation through the JNK and the Wingless signaling pathways. Dev Cell *7*, 491-501.

Sapir, A., Choi, J., Leikina, E., Avinoam, O., Valansi, C., Chernomordik, L. V., Newman, A. P., and Podbilewicz, B. (2007). AFF-1, a FOS-1-regulated fusogen, mediates fusion of the anchor cell in C. elegans. Dev Cell *12*, 683-698.

Scheffner, M., and Staub, O. (2007). HECT E3s and human disease. BMC Biochem *8 Suppl 1*, S6.

Schile, A. J., Garcia-Fernandez, M., and Steller, H. (2008). Regulation of apoptosis by XIAP ubiquitin-ligase activity. Genes Dev *22*, 2256-2266.

Shaham, S., and Horvitz, H. R. (1996a). An alternatively spliced C. elegans ced-4 RNA encodes a novel cell death inhibitor. Cell *86*, 201-208.

Shaham, S., and Horvitz, H. R. (1996b). Developing Caenorhabditis elegans neurons may contain both cell-death protective and killer activities. Genes Dev *10*, 578-591.

Shapiro, P. J., Hsu, H. H., Jung, H., Robbins, E. S., and Ryoo, H. D. (2008). Regulation of the Drosophila apoptosome through feedback inhibition. Nat Cell Biol *10*, 1440-1446.

Smith, D. M., Kafri, G., Cheng, Y., Ng, D., Walz, T., and Goldberg, A. L. (2005). ATP binding to PAN or the 26S ATPases causes association with the 20S proteasome, gate opening, and translocation of unfolded proteins. Mol Cell *20*, 687-698.

Sulston, J. E., and Horvitz, H. R. (1977). Post-embryonic cell lineages of the nematode, Caenorhabditis elegans. Dev Biol *56*, 110-156.

Sulston, J. E., Schierenberg, E., White, J. G., and Thomson, J. N. (1983). The embryonic cell lineage of the nematode Caenorhabditis elegans. Dev Biol *100*, 64-119.

Tait, S. W., de Vries, E., Maas, C., Keller, A. M., D'Santos, C. S., and Borst, J. (2007). Apoptosis induction by Bid requires unconventional ubiquitination and degradation of its N-terminal fragment. J Cell Biol *179*, 1453-1466.

Tateossian, H., Hardisty-Hughes, R. E., Morse, S., Romero, M. R., Hilton, H., Dean, C., and Brown, S. D. (2009). Regulation of TGF-beta signalling by Fbxo11, the gene mutated in the Jeff otitis media mouse mutant. Pathogenetics *2*, 5.

Tsujimoto, Y., Finger, L. R., Yunis, J., Nowell, P. C., and Croce, C. M. (1984). Cloning of the chromosome breakpoint of neoplastic B cells with the t(14;18) chromosome translocation. Science *226*, 1097-1099.

Vaux, D. L., Cory, S., and Adams, J. M. (1988). Bcl-2 gene promotes haemopoietic cell survival and cooperates with c-myc to immortalize pre-B cells. Nature *335*, 440-442.

Voges, D., Zwickl, P., and Baumeister, W. (1999). The 26S proteasome: a molecular machine designed for controlled proteolysis. Annu Rev Biochem *68*, 1015-1068.

Wang, S. L., Hawkins, C. J., Yoo, S. J., Muller, H. A., and Hay, B. A. (1999). The Drosophila caspase inhibitor DIAP1 is essential for cell survival and is negatively regulated by HID. Cell *98*, 453-463.

Wilkinson, H. A., Fitzgerald, K., and Greenwald, I. (1994). Reciprocal changes in expression of the receptor lin-12 and its ligand lag-2 prior to commitment in a C. elegans cell fate decision. Cell *79*, 1187-1198.

Wilson, R., Goyal, L., Ditzel, M., Zachariou, A., Baker, D. A., Agapite, J., Steller, H., and Meier, P. (2002). The DIAP1 RING finger mediates ubiquitination of Dronc and is indispensable for regulating apoptosis. Nat Cell Biol *4*, 445-450.

Yamanaka, A., Yada, M., Imaki, H., Koga, M., Ohshima, Y., and Nakayama, K.-I. (2002). Multiple Skp1-related proteins in Caenorhabditis elegans: diverse patterns of interaction with Cullins and F-box proteins. Curr Biol *12*, 267-275.

Yokokura, T., Dresnek, D., Huseinovic, N., Lisi, S., Abdelwahid, E., Bangs, P., and White, K. (2004). Dissection of DIAP1 functional domains via a mutant replacement strategy. J Biol Chem *279*, 52603-52612.

Yoshida, Y., Chiba, T., Tokunaga, F., Kawasaki, H., Iwai, K., Suzuki, T., Ito, Y., Matsuoka, K., Yoshida, M., Tanaka, K., and Tai, T. (2002). E3 ubiquitin ligase that recognizes sugar chains. Nature *418*, 438-442.

Yuan, J., and Horvitz, H. R. (1992). The Caenorhabditis elegans cell death gene ced-4 encodes a novel protein and is expressed during the period of extensive programmed cell death. Development *116*, 309-320.

Yuan, J., Shaham, S., Ledoux, S., Ellis, H. M., and Horvitz, H. R. (1993). The C. elegans cell death gene ced-3 encodes a protein similar to mammalian interleukin-1 beta-converting enzyme. Cell *75*, 641-652.

Zhong, Q., Gao, W., Du, F., and Wang, X. (2005). Mule/ARF-BP1, a BH3-only E3 ubiquitin ligase, catalyzes the polyubiquitination of Mcl-1 and regulates apoptosis. Cell *121*, 1085-1095.

Zou, H., Henzel, W. J., Liu, X., Lutschg, A., and Wang, X. (1997). Apaf-1, a human protein homologous to C. elegans CED-4, participates in cytochrome c-dependent activation of caspase-3. Cell *90*, 405-413.